JUN 1957 26

REGISTERED No. M. 3121

UNIVERSITY OF MICHIGAN

JUN 25 1957

PHYSICS LIBRARY

PROCEEDINGS

OF THE

INDIAN ACADEMY OF SCIENCES

VOL. XLV] *SECTION A* [No. 4

APRIL 1957

Price Rs. 2 or 3 Sh. *Annual Subscription Rs. 18*

PRINTED AT THE BANGALORE PRESS, BANGALORE CITY, BY C. VASUDEVA RAO
SUPERINTENDENT AND PUBLISHED BY THE INDIAN ACADEMY OF
SCIENCES, BANGALORE.

ON A TIME OF FLIGHT METHOD OF STUDYING THE VELOCITY DISTRIBUTION OF NEUTRONS FROM DIFFUSING MEDIA

By V. C. Deniz, S. B. D. Iyengar and R. Ramanna

(Atomic Energy Establishment, Trombay, Bombay)

Received January 3, 1957

(Communicated by Dr. H. J. Bhabha, F.R.S., F.A.SC.)

In studying the process of energy loss of neutrons in moderating media, it is necessary to know the equilibrium velocity distribution of the neutrons inside the medium. In the investigation described below, the velocity distribution of slow neutrons emerging from the surfaces of finite moderator assemblies due to a pulse of fast neutrons has been studied at various points outside the assembly along a normal to its surface. The distributions have been investigated theoretically and the experimental results have been connected up with the velocity distributions inside the medium. The energing neutrons at certain distances from the moderator are also of interest, since their mean velocities and intensities are such that they can be used as a source of cooled neutrons.

Theory

Consider a moderator assembly of finite dimensions into which a beam of fast neutrons is pulsed. If we measure the intensity of thermal neutrons emerging from one of the faces of the assembly at various points along a normal to the face and at a time t, after the initial pulse, long enough to ensure that the slowing down process is complete, the intensities besides showing the effects of an attenuation due to the angular distribution will also show an increase due to effects of the time of flight of the neutrons having different velocities. At any given time t, the detector also records neutrons of slower velocities which left the assembly at an earlier time.

The thermal neutron intensity at a given point z outside the medium at time t is given by:

$$I = AF(z)\, e^{-\lambda t} \lambda_t \int_{z/t}^{\infty} v^3 e^{-\left(\frac{z}{v_0}\right)^2} e^{\frac{\lambda z}{v}} \phi(v)\, dv \qquad (1)$$

where

A is some constant;

λ_t is the transport mean free path here considered independent of velocity;

λ is the time decay constant of the thermal neutron density inside the assembly;

v_0 is the most probable velocity of the Maxwellian neutron spectrum inside the medium;

$\phi(v)$ is a correction term for the efficiency of the detector; and

$F(z)$ is a correction factor due to angular distribution arising from the last collision effects discussed later.

The integration is carried out from z/t to ∞ since no neutrons of velocity less than z/t will have arrived at the detector.

Let us write

$$I = KF(z)\, e^{-\lambda t}\, e^{\frac{\lambda z}{v_m}} \tag{2}$$

where we define a mean velocity v_m as follows:

$$e^{\frac{\lambda z}{v_m}} = \frac{\int_{z/t}^{\infty} v^3 e^{-\left(\frac{v}{v_0}\right)^2} e^{\frac{\lambda z}{v}}\, dv}{\int_{z/t}^{\infty} v^3 e^{-\left(\frac{v}{v_0}\right)^2}\, dv} \tag{3}$$

The actual mean velocity of the neutron flux at a point z is given by

$$\bar{v} = \frac{\int_{z/t}^{\infty} v^4 e^{-\left(\frac{v}{v_0}\right)^2} e^{\frac{\lambda z}{v}} dv}{\int_{z/t}^{\infty} v^3 e^{-\left(\frac{v}{v_0}\right)^2} e^{\frac{\lambda z}{v}} dv} \tag{4}$$

For abbreviation, the integrals

$$\int_{z/t}^{\infty} v^4 e^{-\left(\frac{v}{v_0}\right)^2} e^{\frac{\lambda z}{v}}\, dv, \int_{z/t}^{\infty} v^3 e^{-\left(\frac{v}{v_0}\right)^2} e^{\frac{\lambda z}{v}}\, dv \text{ and } \int_{z/t}^{\infty} v^2 e^{-\left(\frac{v}{v_0}\right)^2} e^{\frac{\lambda z}{v}} dv$$

will be denoted by I_{v^4}, I_{v^3} and I_{v^2} respectively.

It can be shown that

$$\int_0^s I_{v^3} dz = \frac{e^{\lambda t}}{\lambda} \int_0^{z/t} v^4 e^{-\left(\frac{v}{v_0}\right)^2} dv - \frac{1}{\lambda} \int_0^{\infty} v^4 e^{-\left(\frac{v}{v_0}\right)^2} dv + \frac{1}{\lambda} \int_{z/t}^{\infty} v^4 e^{-\left(\frac{v}{v_0}\right)^2} e^{\frac{\lambda z}{v}} dv$$

$$\therefore \quad \int_0^s I_{v^3} dz = \frac{1}{\lambda} \left[I_{v^4} + P \right] \tag{5}$$

where

$$P = e^{\lambda t} \int_0^{z/t} v^4 e^{-\left(\frac{v}{v_0}\right)^2} dv - \int_0^{\infty} v^4 e^{-\left(\frac{v}{v_0}\right)^2} dv$$

$$= e^{\lambda t} v_0^5 \left[\frac{3\sqrt{\pi}}{8} \operatorname{erf} x - \tfrac{1}{2} x^3 e^{-x^2} - \tfrac{3}{4} x e^{-x^2} \right] - \frac{3\sqrt{\pi}}{8} v_0^5$$

and

$$x = \frac{z}{t v_0}$$

From (2) and (3) we have

$$I = \frac{KF(z)\, e^{-\lambda t} I_{v^3}}{\frac{v_0^4}{2} (1 + x^2)\, e^{-x^2}} \tag{6}$$

Since

$$\int_{z/t}^{\infty} v^3 e^{-\left(\frac{v}{v_0}\right)^2} dv = \frac{v_0^4}{2} (1 + x^2)\, e^{-x^2}$$

From (3) and (5) we have

$$\frac{v_0^4}{2} \int e^{\frac{\lambda z}{v_m}} (1 + x^2)\, e^{-x^2} dz = \frac{1}{\lambda} (I_{v^4} + P)$$

$$\therefore \quad \bar{v} = \frac{I_{v^4}}{I_{v^3}} = \frac{\frac{\lambda v_0^4}{2} \int_0^s e^{\frac{\lambda z}{v_m}} (1 + x^2)\, e^{-x^2} dz - P}{\frac{v_0^4}{2} e^{\frac{\lambda z}{v_m}} (1 + x^2)\, e^{-x^2}} \tag{7}$$

In the region of investigation z is between 10 cm. and 30 cm. and t is 700 microseconds. In these regions the terms containing z/t can be neglected

and the mean velocity of the neutrons at various points from the moderator is given by

$$\bar{v} = v_m\left(1 - e^{\frac{\lambda s}{v_m}}\right) + \frac{3\sqrt{\pi}}{4}\, v_0 e^{\frac{\lambda s}{v_m}} \tag{8}$$

For a thin detector the mean has to be taken over the density spectrum and is given by

$$\bar{v} = v_{m'}\left(1 - e^{\frac{\lambda s}{v_{m'}}}\right) + \frac{2}{\sqrt{\pi}}\, v_0 e^{\frac{\lambda s}{v_{m'}}} \tag{8 a}$$

where $v_{m'}$ is similar to v_m defined in (3), but taken over the density spectrum.

DETERMINATION OF v_0

From (3) we have

$$I_{v^3} = \frac{v_0^4}{2}\, e^{\frac{\lambda s}{v_m}} (1 + x^2)\, e^{-x^2}$$

I_{v^3} can be either numerically integrated or within limits depending on the value of z be determined for various values of v_0 from the following expression:

$$\begin{aligned} I_{v^3} &= \int_{s/t}^{\infty} v^3 e^{-\left(\frac{v}{v_0}\right)^2} e^{\frac{\lambda s}{v}}\, dv \\ &= \int_{s/t}^{\infty} v^3 e^{-\left(\frac{v}{v_0}\right)^2} \left(1 + \frac{\lambda z}{v} + \frac{\lambda^2 z^2}{2v^2} + \ldots.\right) dv \\ &= \int_{s/t}^{\infty} v^3 e^{-\left(\frac{v}{v_0}\right)^2} dv + \lambda z \int_{s/t}^{\infty} v^2 e^{-\left(\frac{v}{v_0}\right)^2} dv \\ &\qquad + \frac{\lambda^2 z^2}{2} \int_{s/t}^{\infty} v e^{-\left(\frac{v}{v_0}\right)^2} dv + \ldots. \end{aligned} \tag{9}$$

Fig. 2 shows the function $v^3 e^{-\left(\frac{v}{v_0}\right)^2} e^{\frac{\lambda s}{v}}$

If a thin detector is used, the function becomes $v^2 e^{-\left(\frac{v}{v_0}\right)^2} e^{\frac{\lambda s}{v}}$

This and the function in the case of an intermediate detector are also shown.

It can be seen that each of these functions goes through a dip. If in the integrals of these functions, the lower limit is chosen to lie in the dip region, the integral will not be sensitive to the actual value of the limit. This is particularly true for small values of z.

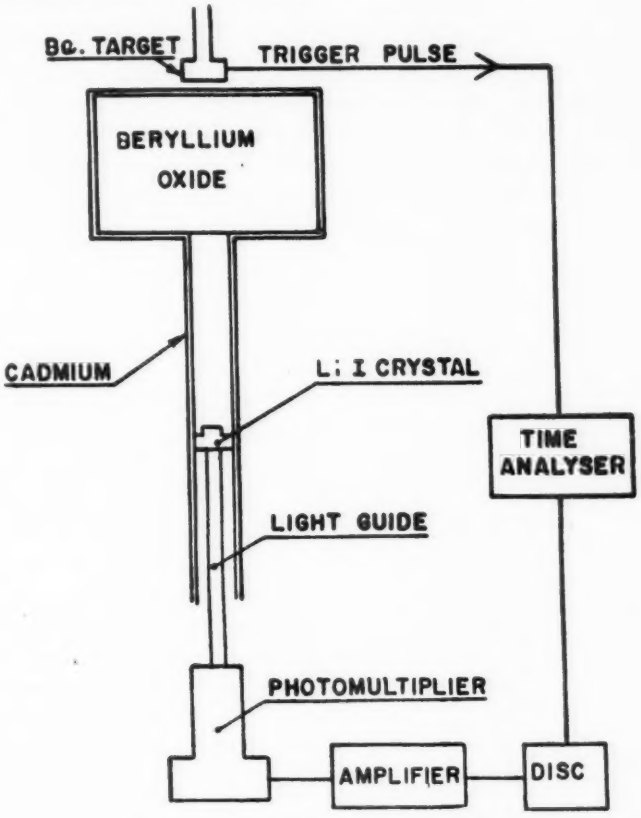

FIG. 1. Block Diagram of Expt. Arrangement

In order to compare the theory with experiment, it is necessary to take into account the following correction factors. Firstly, the neutrons are emitted not from a point but from a finite surface area of the moderator and in the experiment this area was circular. Secondly the neutrons are not emitted isotropically but have an angular distribution due to the last collision effects. Fermi[1] has derived the following expression for the angular distribution of neutrons emerging from an infinite plane surface:

$$f(\theta) \propto \cos\theta\,(1 + \sqrt{3}\cos\theta) \qquad (10)$$

It is assumed that the expression is not appreciably altered due to the finite size of the assembly used in the experiment. Since neutrons from only a small surface area are detected, the second term in (10) does not contribute appreciably to the correction factor. Hence the distribution approximates to a pure cosine law.

It is also necessary to take into consideration the fact that the neutrons are emitted, on the average, not from the actual boundary of the assembly but from various points inside where they had their last collision. This is done by assuming that they are emitted from a layer inside the medium one transport mean free path from the boundary.

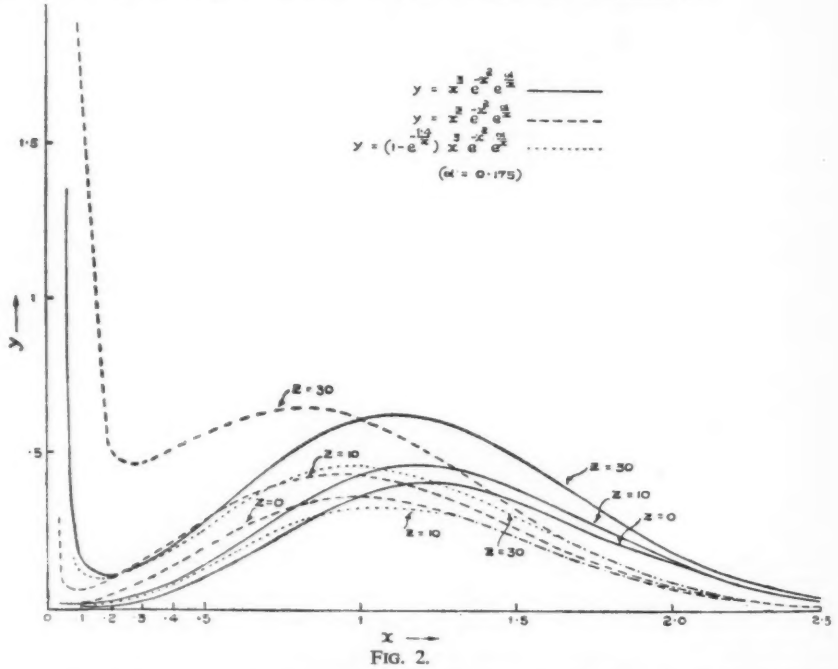

FIG. 2.

Taking into account these various factors, the intensity is now given by

$$I = Ce^{-\lambda t}\lambda_t \int_0^{\infty}\int_0^{R} v^3 e^{-\left(\frac{v}{v_0}\right)^2} e^{\frac{\lambda\alpha}{v}} \frac{\cos^2\theta}{r^2}\,\rho d\rho dv \qquad (11)$$

where

$$r^2 = \rho^2 + (z + \lambda_t)^2$$

and R is the radius of the area emitting neutrons.

The correction factor is mainly due to the angular distribution. The time of flight correction is small since the actual flight paths from various points of the surface to the detector are not very different. The integral (11) becomes

$$I = Ke^{-\lambda t}e^{\frac{\lambda s}{v_m}}\left[\frac{1}{2}\left\{1 - \frac{1}{1 + \frac{R^2}{(z+\lambda t)^2}}\right\}\right] \tag{12}$$

The time of flight correction in detectors used in pulsed neutron work is discussed by Von Dardel.[2]

(12) gives the geometrical correction factor $F(z)$ introduced in (1).

$$F(z) = \frac{1}{2}\left\{1 - \frac{1}{1 + \frac{R^2}{(z+\lambda t)^2}}\right\} \tag{13}$$

Experimental Arrangement

The arrangement used in the experiment was the same as that used by Ramanna *et al.*,[3] and is shown in Fig. 1. The beryllium oxide was available in the form of blocks $10 \times 10 \times 5$ cm.^{3} and these were stacked up to give the required sizes. Two sizes were used $20 \times 20 \times 20$ cm.^{3} and $20 \times 40 \times 40$ cm.^{3}

The medium was covered on all sides with 0·5 mm. thick cadmium leaving a circular opening of radius 3·75 cm. in the centre of the bottom face. A cylindrical tube made of cadmium of this radius and 50 cm. length was placed at this opening with its axis perpendicular to the surface. The neutrons emerging into the tube were detected by a LiI crystal capable of being positioned at various points along the axis of the tube. The crystal was of 0·5″ diameter and 1 cm. thick.

The scintillation pulses from the crystal were taken along a perspex light guide and detected by means of a 6262 photomultiplier. The photomultiplier pulses were then fed into a ten channel time analyser and also into a scalar which recorded the integrated counts within the required time range.

Discussion of Results

Fig. 3 shows log plots of I_{v^3} and I_{v^2} against z. It will be seen that both the plots, particularly the log I_{v^3} plot, are straight lines for values of z less than 30 cm. On the same figure a plot of I_{v^4}/I_{v^3} against z is also given. Fig. 4 shows the log plots of I_v against z for two values of λ,

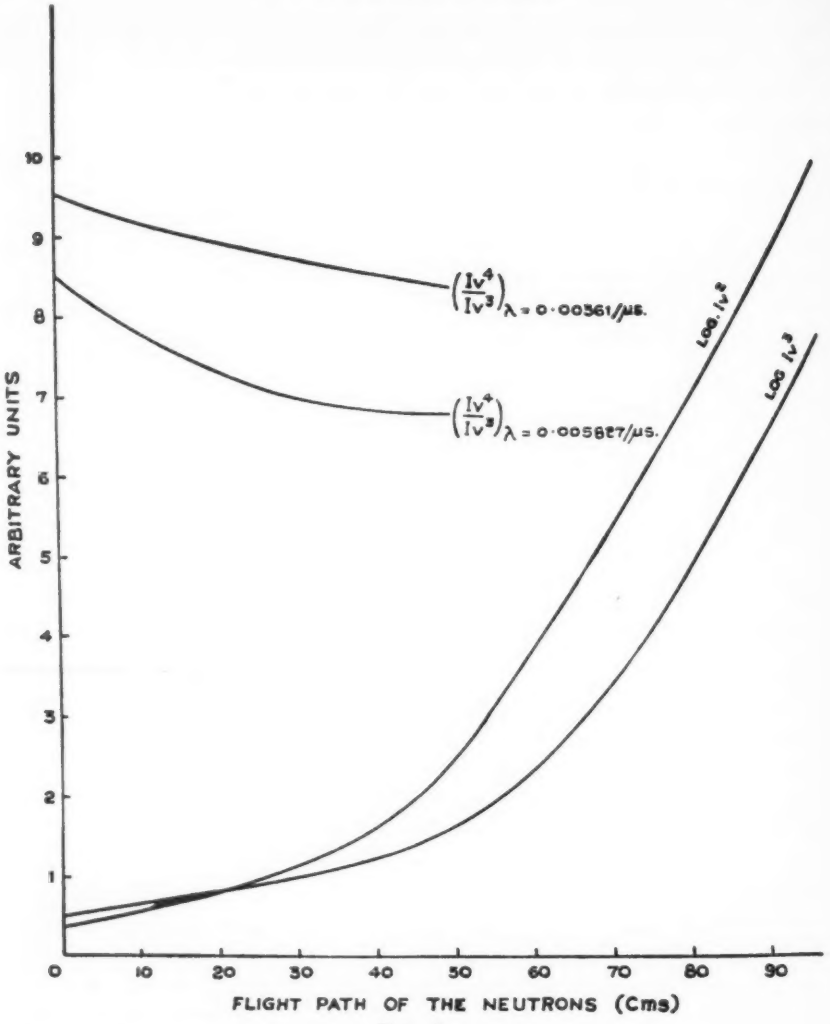

FIG. 3.

0·00361 and 0·005827 and for each of them for two values of v_0, 0·20 and 0·18 and 0·20 and 0·16 cm./microsecond respectively. Here a correction has also been applied for the variation of detector efficiency with neutron velocity. This is done by introducing a factor $(1 - e^{-\alpha s/v})$ where s is the thickness of the crystal, $\alpha = N\sigma_1 v_1$, where N is the number of atoms of Li per c.c., σ_1 is the absorption cross-section of Li at some velocity v_1, and $\bar{v}$

is the mean velocity of the flux spectrum given by (8). This correction varies with distance since it is dependent on $\bar{v}$.

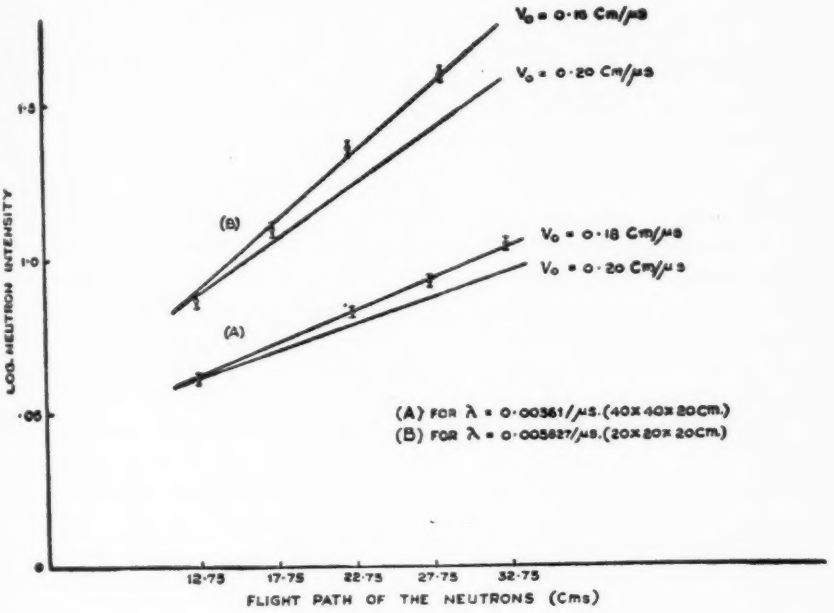

FIG. 4.

The λ's were selected from the measured values[4] for the two sizes of beryllium oxide assemblies $20 \times 40 \times 40$ cm.[3] and $20 \times 20 \times 20$ cm.[3] respectively, for which the experiment was performed. The cut-offs were determined by taking the exponential mean of 400 and 1200 microseconds, the beginning and the end of the time interval for which the counts were taken. In all these plots, z is the value of the flight path, given by the sum of λ_t and the distance from the surface of the moderator. The experimental points are also shown on the same figure after suitable normalisation. It will be seen that the experimental points agree with values for v_0 of approximately 0·18 and 0·16 cm./microsecond respectively for the two sizes. Measurements of the diffusion cooling constant in beryllium oxide[4] give values for v_0 of approximately 0·19 and 0·17 cm./microsecond respectively. The agreement can be considered as good, since the experimental errors and the errors due to approximations in the theory are more than the differences in the values of v_0. It is seen that due to "diffusion cooling"

the most probable velocity of the neutrons in the moderator is very much less than the most probable velocity corresponding to the temperature of the moderator, *i.e.*, 0·22 cm./microsecond.

It will be seen from Fig. 3 that due to time of flight effects, the flux spectrum shows considerable cooling. For $\lambda = 0{\cdot}005827$ microsecond at $z = 30$ cm. the mean velocity is cooled by about 10%. The density spectrum is even more rapidly cooled. This fact can be of possible use in obtaining cooled neutrons for cross-section experiments.

We wish to thank Mr. G. S. Mani for numerous helpful suggestions and discussions throughout the course of the work. Our thanks are also due to Mr. N. Umakantha for many helpful suggestions and discussions and to Messrs. M. P. Navalkar, S. K. Ambardekar, F. R. Bhathena and P. N. Rama Rao, for running the cascade generator and for their help in taking readings.

REFERENCES

1. Fermi .. *Ric. Sci.*, 1936, **7**, 13.
2. Von Dardel, G. F. .. *Thesis Goteborg*, 1953.
3. Ramanna, R., Mani, G. S., Iyengar, P. K., Iyengar, S. B. D. and Joshi, B. V. *J. Nuclear Energy*, 1956, **2**, 145.
4. Ramanna, R., *et al.* (unpublished).

SLOWING DOWN AND DIFFUSION OF NEUTRONS IN BERYLLIUM OXIDE

By S. B. D. Iyengar, G. S. Mani, R. Ramanna and N. Umakanth

(Atomic Energy Establishment, Trombay, Bombay)

Received January 3, 1957

(Communicated by Dr. H. J. Bhabha, F.R.S., F.A.SC.)

Introduction

Pulsed neutron techniques offer a powerful method for the study of the characteristics of the slowing down of neutrons just before they attain equilibrium.[1,2] In using these techniques two procedures are possible. The decay rate of thermal neutrons in a finite assembly due to an initial instantaneous burst of fast neutrons could be studied and would furnish information regarding the rate of approach to equilibrium in the last stages of slowing down. The instantaneous neutron energy at various times could also be determined directly by transmission through $1/v$ absorbers. In this paper results obtained for Beryllium oxide using the first method are reported.

Theory

Unlike in infinite moderators where the neutrons attain, at equilibrium, the moderator temperature, in finite assemblies, the equilibrium temperature of the neutrons is lower than the moderator temperature. This is because the higher energy part of the neutron spectrum is more depleted than the lower energy part due to differential leakage from the assembly, the leakage being, in the first approximation, proportional to the neutron velocity.

In what follows we shall use T_p to represent the equilibrium temperature of the neutrons and T_0 for the moderator temperature.

The thermal neutron density at a point r, and at time t, when the contribution due to the higher harmonics is negligible, is given by

$$\rho(r, t) = A(r') B(r) e^{-[\tau - D(T_p)\tau_{cs}]\omega^2} e^{-\lambda t}$$

$$= k(r', r, T_p) e^{-\lambda t} \qquad (1)$$

and

$$\lambda = \frac{1}{\tau_{cs}} + D(T_p)\omega^2$$

where $A(r')$ and $B(r)$ are functions of the source and the detector positions; τ is the age of the source neutrons to the equilibrium temperature; $D(T_p)$ is the diffusion coefficient of neutrons at temperature T_p; τ_{cs} is the mean life time of these neutrons in an infinite assembly; ω^2 is the geometrical buckling.

The equilibrium temperature T_p, as mentioned above, is a function of the moderator size, that is of ω^2, and to a first approximation we can write

$$D(T_p) = D(T_0) - C\omega^2 \tag{2}$$

where C is called the diffusion cooling constant. By measuring the decay rate λ for various sizes of the moderator, it is possible to determine $D(T_0)$, τ_{cs} and C.

As can be seen from equation (1), the amplitude term contains the exponential factor $\exp.[-(\tau - D(T_p)\tau_{cf})\omega^2]$ which depends on the size of the moderator. If for various sizes of the moderator the source and the detector terms $A(r')$ and $B(r)$ are calculated, the constant $[\tau - D(T_p)\tau_{cf}]$ can be determined.

The total energy loss of neutrons at time t is composed of energy loss due to collisions, energy loss due to leakage and energy loss due to absorption. If the absorption cross-section varies as $1/v$, then the energy loss due to absorption would not change the average energy of the neutrons as can be seen below. The rate of decay of the total number of neutrons in the system depends only on the leakage and absorption.

Let $A(t)f(E)\,dE$ be the number of neutrons at time t having energy between E and $E + dE$. $f(E)\,dE$ is normalised such that $A(t)$ represents the total number of neutrons at time t, that is

$$\int_0^\infty f(E)\,dE = 1. \tag{3}$$

Then the equation describing the rate of total energy loss is given by

$$\begin{aligned} -\frac{d}{dt}\left[A(t)\int_0^\infty Ef(E)\,dE\right] &= \sqrt{\frac{2}{m}}\,A(t)\int_0^\infty \Sigma_t(E)\,\langle E\rangle_{AV}E^{\frac{1}{2}}f(E)\,dE \\ &+ \sqrt{\frac{2}{m}}\,\frac{\omega^2}{3}\,A(t)\int_0^\infty \lambda_t(E)\,E^{3/2}f(E)\,dE \\ &+ \sqrt{\frac{2}{m}}\,A(t)\int_0^\infty \Sigma_a(E)\,E^{3/2}f(E)\,dE \end{aligned} \tag{4}$$

and that describing the rate of decay of the total number of neutrons i the system is given by

$$-\frac{d}{dt}\mathrm{A}(t) = \sqrt{\frac{2}{m}}\,\frac{\omega^2}{3}\,\mathrm{A}(t)\int_0^\infty \lambda_t(\mathrm{E})\,\mathrm{E}^{\frac{1}{2}} f(\mathrm{E})\,d\mathrm{E} + \sqrt{\frac{2}{m}}\,\mathrm{A}(t)\int_0^\infty \Sigma_a(\mathrm{E})\,\mathrm{E}^{\frac{1}{2}} f(\mathrm{E})\,d\mathrm{E} \tag{5}$$

Here $<\mathrm{E}>_{\mathrm{AV}}$ is the average energy lost by a neutron having energy between E and $\mathrm{E}+d\mathrm{E}$ in one collision, $\lambda_t(\mathrm{E}) = 1/\Sigma_t(\mathrm{E})$ is the transport mean free path for neutron of energy E, $\Sigma_a(\mathrm{E})$ is the microscopic absorption cross-section for neutrons having the energy E, and m is the mass of the neutron.

We define the average energy $\bar{\mathrm{E}}(t)$ at time t as

$$\bar{\mathrm{E}}(t) = \int_0^\infty \mathrm{E} f(\mathrm{E})\,d\mathrm{E} \tag{6}$$

Then from (4), (5) and (6), assuming Σ_a (E) to vary as $1/v$, we get

$$-\frac{d\bar{\mathrm{E}}(t)}{dt} = \sqrt{\frac{2}{m}}\int_0^\infty <\mathrm{E}>_{\mathrm{AV}}\ \Sigma_t\ (\mathrm{E})\,\mathrm{E}^{\frac{1}{2}} f(\mathrm{E})\,d\mathrm{E} + \sqrt{\frac{2}{m}}\,\frac{\omega^2}{3}\int_0^\infty \lambda_t(\mathrm{E})\,\mathrm{E}^{\frac{1}{2}}\left(\mathrm{E}-\bar{\mathrm{E}}(t)\right) f(\mathrm{E})\,d\mathrm{E} \tag{7}$$

It can be shown that, both on the Debye model[4] and on the gas model,[5] when the neutron temperature is a few hundred degrees above the moderator temperature

$$\sqrt{\frac{2}{m}}\int_0^\infty <\mathrm{E}>_{\mathrm{AV}}\ \Sigma_t(\mathrm{E})\,\mathrm{E}^{\frac{1}{2}}\ f(\mathrm{E})\,d\mathrm{E} \approx \gamma\,[\bar{\mathrm{E}}(t) - \mathrm{E}_0] \tag{8}$$

where E_0 is the mean energy of the moderator atoms. γ is a constant which depends mainly on the Debye temperature, the scattering cross-section and the moderator temperature.

We assume that $\lambda_t(\mathrm{E})$ is independent of energy, which is approximately true for neutron temperatures a few hundred degrees above the moderator temperature. We further assume that the neutron spectrum in this region is Maxwellian, an assumption that is true only for large sizes. Then we get

$$\sqrt{\frac{2}{m}}\,\frac{\omega^2}{3}\int_0^\infty \lambda_t(\mathrm{E})\,\mathrm{E}^{\frac{1}{2}}\,[\mathrm{E}-\bar{\mathrm{E}}(t)]\,f(\mathrm{E})\,d\mathrm{E} = \frac{\mathrm{D}(t)\,\omega^2}{3}\,\bar{\mathrm{E}}(t) \tag{9}$$

where

$$D(t) = \frac{\lambda_t \bar{v}(t)}{3},$$

$\bar{v}(t)$ being the mean neutron velocity corresponding to the energy $\bar{E}(t)$. Combining (7), (8) and (9) and using the relation $\bar{E} = 3/2\,kT$, T being the temperature of the neutrons, we get

$$-\frac{dT}{dt} = \frac{D(T)\,\omega^2}{3}\,T + \gamma(T - T_0) \tag{10}$$

For equilibrium temperature T_p, since $dT_p/dt = 0$, we get

$$\frac{D(T_p)\,\omega^2}{3}\,T_p + \gamma(T_p - T_0) = 0 \tag{11}$$

For an infinite size ($\omega^2 = 0$) we get, from (10) and (11)

$$-\frac{dT}{dt} = \gamma(T - T_0); \quad T_p = T_0 \tag{12}$$

Integrating (12) we get

$$T(t) - T_0 = Ae^{-\beta t}; \quad \beta = \gamma \tag{13}$$

That is, the neutrons attain thermal equilibrium exponentially in time with the relaxation time given by β^{-1}.

For a large finite moderator, ($\omega^2 \approx 0$ and $T_p \approx T_0$) equation (11) would yield, when the neutron energy is very near the equilibrium energy, the following solution:

$$T(t) - T_p = Ae^{-\beta t}$$

$$\beta = \frac{D\omega^2}{3} + \gamma \tag{14}$$

Now we shall relate the constant γ to the diffusion cooling constant C which is defined by

$$D(T_p) = D(T_0) - C\omega^2$$

Since $D(T) = \lambda_t \bar{v}(T)/3$, where $\bar{v}(T)$ is the mean velocity of neutrons having temperature T, we get

$$\frac{C\omega^2}{D(T_0)} = 1 - \left(\frac{T_p}{T_0}\right)^{\frac{1}{2}} \tag{15}$$

where it is assumed λ_t to be a constant. Since from experiments we determine C and D (T_0), T_p could be obtained for any size ω^2 from (15) and using (11) we get γ. For large sizes, $T_p \approx T_0$, we get the simple formula

$$\gamma = \frac{D^2(T_0)}{6C} x \tag{16}$$

where x is the correction for the change of λ_t with energy. For Beryllium oxide $x \approx 1$.

From (8), assuming λ_t to be constant and the neutron spectrum to be Maxwellian, we get

$$|<E>|_{AV} = \gamma \frac{\bar{E} - E_0}{\Sigma_t \bar{v}} \tag{17}$$

where $|<E>|_{AV}$ is the mean loss of energy per collision, averaged over the neutron spectrum, for neutrons having a mean energy $\bar{E}$ and a mean velocity $\bar{v}$. Hence $|<E>|_{AV}$ could be determined experimentally from the values of C and compared with theory.

Experimental Arrangements

The experimental arrangement was the same as described in I[6]. The fast neutron bursts were produced from the $Be^9(d, n)B^{13}$ reaction in a Cascade Generator by pulsing the extraction voltage of the R.F. ion source. The pulsing frequency was 550 per second and the neutron bursts had a duration of about 25 microsecond. The thermal neutrons were detected by a LiI crystal and analysed by a ten channel time analyser described elwewhere.[7] A Stilbene scintillator was used as a fast neutron monitor to normalise the source strength of the neutron bursts. The neutrons were counted after an initial delay so adjusted that the contribution from higher harmonics was less than 1%.

The Beryllium oxide assembly was surrounded on all sides by Cadmium followed by paraffin to prevent the leakage neutrons from re-entering the system.

Results

Fifteen different sizes of the assembly were used and the decay rate was obtained for each of them by the method of least squares. The error due to statistical fluctuations in the counting rate was of the order of $\cdot 005\,\lambda$ while the instrumental error was estimated to be approximately $\cdot 02\,\lambda$.

Fig. 1 shows the parabola obtained by plotting λ against ω^2. By the method of least squares, the values of $D(T_0)$, τ_{cs} and C were obtained and these are given in Table I. The errors quoted in the table are the estimated experimental errors.

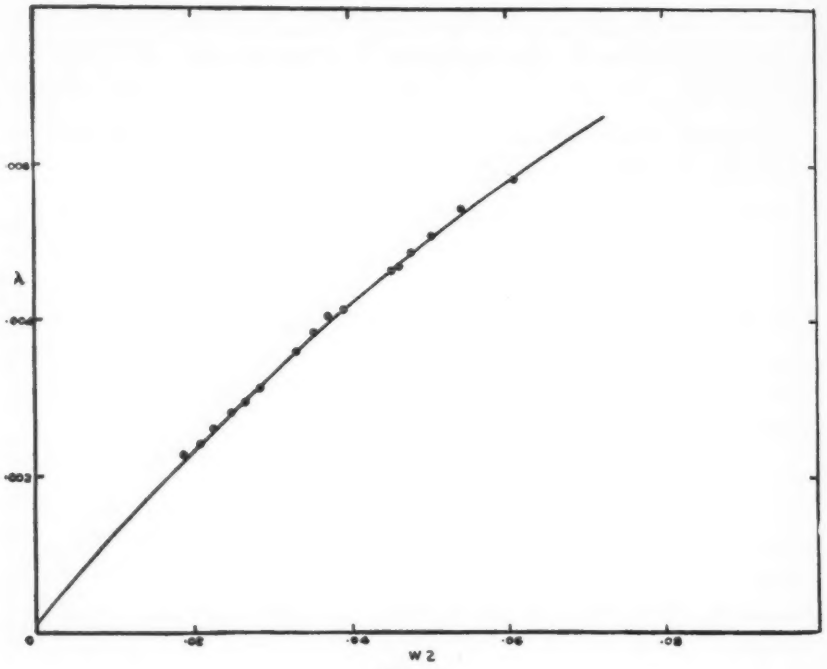

FIG. 1.

TABLE I

Slowing down and diffusion constants of BeO at 24° C.

Mean density of BeO	.. ..	2·96 cm./c.c.
Temperature T_0	.. ..	297° K.
Diffusion coefficient, $D(T_0)$	..	$0{\cdot}118 \pm 0{\cdot}002$ cm.$^2/\mu s$.
Diffusion time τ_{cs}	.. ..	$7600 \pm 150\,\mu s$.
Diffusion length L	.. ..	$29{\cdot}9 \pm {\cdot}6$ cm.
Diffusion cooling constant C	..	$0{\cdot}385 \pm 0{\cdot}008$ cm.$^2/\mu s$.
$(\tau - D\tau_{cf})$	.. .. ..	73 ± 3 cm.^{2}
'Slowing down time'	.. ..	τ_{cf} ($\tau = 100$ cm.^{2}) 230 ± 30

Using the fast neutron monitor, the normalised amplitude terms for various sizes were obtained and from these, the value of $[\tau - D\tau_{cf}]$ was determined, assuming first collision effects to be negligible (Fig. 2). These effects would have caused a change in the exponential character of the variation of the amplitude term with ω^2 when the direct path length is varied by changing the source and the detector positions. It was confirmed that within experimental errors this effect is negligible. The quantity $\tau - D\tau_{cf}$ was found to be 73 ± 3 cm.^{2} Assuming an age of 100 cm.^{2} for Beryllium oxide, and that $D(T_p) \approx D(T_0)$, it was found that $\tau_{cf} = 230 \pm 30\,\mu s$.

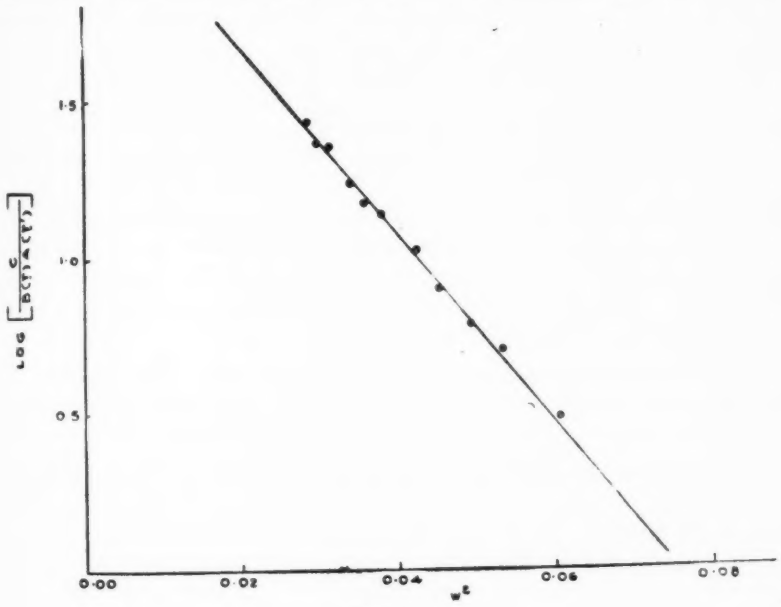

FIG. 2.

In Table II are given the values of the relaxation time β^{-1} derived from the value of C using equation (13). For comparison the values for other substances are also given.

DISCUSSION

It will be seen from Table II that the relaxation time β^{-1} for an infinite BeO assembly, as calculated from the value of C, is $165 \pm 10\,\mu s$. Singwi and Kothari,[4] using the Debye model have obtained for an infinite Beryllium asembly, a value of $20\,\mu s$ for the relaxation time. Since the Debye temperatures of Beryllium and BeO are of the same order, th relaxation time in

TABLE II*

	Water†	Graphite†	Beryllium†	Beryllium Oxide		
Density gm./c.c.	1·00	1·78	1·67	2·96		
C cm.$^4/\mu s$	0·004±0·001	1·2 ±0·19	0·3 ±0·1	0·385±0·008		
D (T_0) cm.^{2}	0·035±0·001	0·198±0·003	0·122±0·005	0·118±0·002		
Size	Infinite	Infinite	Infinite	Infinite	40×40×40 cm.^{3}	20×20×20 cm.^{3}
β^{-1} μs	20±38	183±38	121±50	165±10	150±8	119±6

* All these constants refer to a temperature of 24° C.

† Constants of these materials are taken from Reference 8. β^{-1} for graphite has been obtained by transmission experiments in Reference 2 and the value quoted is 200 ± 25 μs.

these materials should not be very different, as also seen from Table II. It is very interesting to note that the Debye model yields a very low value for the relaxation time.[4] Antonov *et al.*[2] using both the transmission and the diffusion methods have measured the relaxation time in Graphite and obtained a value of the order of 200 μs.

It can be seen from Table II, that the relaxation time decreases with decrease in the size of the assembly showing that the neutrons reach equilibrium much faster in finite assemblies than in an infinite assembly.

The value of the diffusion length L obtained here for BeO agrees with that obtained by Ramanna *et al.*,[6] but is less than the value of 32·7 cm. obtained by Kochelin *et al.*[9] using the static method. A value of 10·3 ± ·2 barns for σ_s is obtained from our value of λ_t using the relation $\sigma_t = \sigma_s(1 - \cos\theta)$ and for σ_a we get the value of 8·37 ± mb. at 2200 metres/sec. for this sample of BeO.

Our thanks are due to Mr. M. P. Navalkar and to Mr. F. R. Bathena for their help with the electronics and to Mr. S. K. Amberdakar for his help with the accelerator.

REFERENCES

1. Von Dardel .. *Phys. Rev.*, 1954, **94**, 1272.
2. Antonov, A. V., Bergman, A. E., Isakov, A. I., Murin, I. D. and Neupokov, B. A. (Private communication.) Part of this paper was read at the Geneva Conference, 1955.
3. Iyengar, S. B. D. and Mani, G. S. *Proc. Ind. Acad. Sci.*, 1955, **42**, 175.

4. Kothari, L. S. and Singwi, K. S. — *Curr. Sci.*, 1956, **25**, 286.

5. Von Dardel .. — "The interactions of neutrons with matter studied with a pulsed neutron source," *Thesis* (Goetberg).

6. Ramanna, R., Mani, G. S., Iyengar, P. K., Iyengar, S. B. D. and Joshi, B. V. — *J. Nuclear Energy*, 1956, **2**, 145.

7. Iyengar, P. K. .. — *J. Sci. Ind. Res.*, 1956, **15 A** (9).

8. Antonov, A. V., Isakov, A. I., Murin, I. D., Neupokov, B. A., Frank, I. M., Shapiro, F. L. and Stranich, I. V. — "A study of neutron diffusion in beryllium, graphite and water using the impulse method". Paper presented at the Geneva Conference, 1955.

9 Kochelin, J. C., Martely, J. and Duggal, V. P. — "Measurement of diffusion length of thermal neutrons in BeO," Paper presented at the Geneva Conference, 1955.

TEMPERATURE DEPENDENCE OF THE SLOWING DOWN AND DIFFUSION CONSTANTS OF NEUTRONS IN BERYLLIUM OXIDE

By S. B. D. Iyengar, G. S. Mani, R. Ramanna and N. Umakanth

(*Atomic Energy Establishment, Trombay, Bombay*)

Received January 3, 1957

(Communicated by Dr. H. J. Bhabha, F.R.S., F.A.SC.)

Introduction

It has been pointed out in a previous paper[1] that the slowing down and diffusion constants in moderators give information regarding the rate of approach to equilibrium of neutrons in the last stages of the slowing down process. From a measurement of the temperature dependence of these constants it is possible to verify the theory of slowing down in crystalline media. In this paper we report the results of experiments on the temperature dependence of the diffusion coefficient D and the diffusion cooling constant C of Beryllium oxide in the range between 300° K. and 450° K. using the pulsed neutron technique. The relaxation slowing down time at room temperature has been determined using the transmission method and it was found to agree with that obtained in reference (1).

Determination of Temperature Dependence of C and D

The experimental arrangement was the same as described in reference (1). The Beryllium oxide was heated in an electric furnace. In order to prevent the neutrons which escape from the assembly from re-entering, the furnace was surrounded by paraffin on all sides and by blocks of wood at the top and at the bottom and the Beryllium oxide assembly was covered on all sides by cadmium sandwiched between two thin aluminium sheets. An automatic pyrometer control connected to two thin copper—constantan thermocouples in series, one placed at the centre and the other at the edge of the assembly, measured and controlled the temperature of the furnace. Since Beryllium oxide has a fairly high thermal conductivity, steep temperature gradients were assumed not to exist in the assembly and sufficient time was allowed for the temperature to become uniform. The uncertainty in the temperature measuremtent was of the order of 5%. A thin aluminium sheet was used to shield the assembly from receiving direct radiations from

the filaments of the furnace. This helped to reduce any temperature gradient that might have existed and also prevent the cadmium from melting.

The detector was cooled by circulating cold water. Since the efficiency of the LiI crystal rapidly increases with the decrease of temperature, a thin copper—constantan thermo couple was placed at the top of the crystal so as to be certain that the crystal temperature remains constant throughout the experiment.

The decay of thermal neutrons, after the higher harmonics have died down, is exponential in time with a decay constant given by

$$\lambda(T_0) = \frac{1}{\tau_{cs}} + D(T_0)\,\omega^2 - C(T_0)\,\omega^4 \qquad (1)$$

where

ω^2 is the geometrical buckling,

$D(T_0)$ is the diffusion coefficient,

and $C(T_0)$ the diffusion cooling constant corresponding to the absolute temperature T_0 of the moderator,

τ_{cs} is the mean life-time of thermal neutrons in an infinite moderator.

For moderators having $1/v$ absorption τ_{cs} is independent of moderator temperature. It is seen from (1) that a plot of

$$y(T_0) = \left[\lambda(T_0) - \frac{1}{\tau_{cs}}\right] \Big/ \omega^2$$

against ω^2 for any moderator temperature T_0 is a straight line with a slope $C(T_0)$ and an intercept $D(T_0)$.

It has been shown in reference (1) that the relaxation time β^{-1} is related to $C(T_0)$ and $D(T_p)$ by

$$\beta = \frac{D(T_0)\,\omega^2}{3} + \gamma \qquad (2)$$

and that the equilibrium temperature T_P is given by,

$$\frac{D(T_P)\,\omega^2}{3} T_P + \gamma (T_P - T_0) = 0 \qquad (3)$$

where

$$\gamma = D^2(T_0)/6\ C \qquad (4)$$

γ is the " heat transfer coefficient " and represents the mean energy transferred to the system by a neutron for unit energy difference between the neutron and the system.

The decay constants for different sizes at temperatures, 80° C. and 140° C., were determined. Using the value of 7660 μs for τ_{cs} obtained in reference (1),

$$Y(T_0) = \left[\lambda(T_0) - \frac{1}{\tau_{cs}}\right] \Big/ \omega^2$$

was calculated and plotted against ω^2 (Figs. 1 and 2). The values of $C(T_0)$ and $D(T_0)$ are given in Table I for different temperatures. In Table II the values of β^{-1} for various sizes and temperatures, as calculated from the values of C and D, are given.

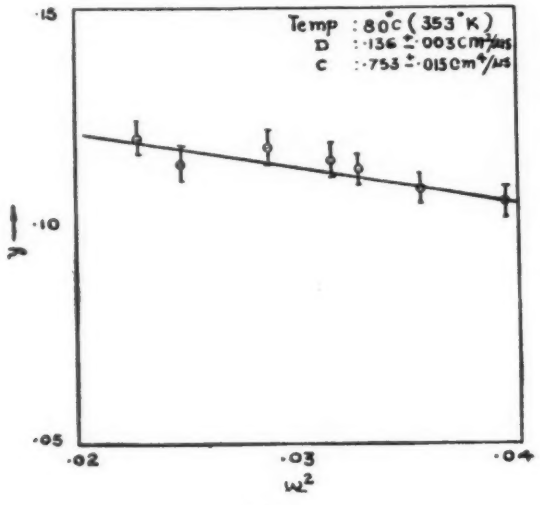

FIG. 1.

TABLE I

Values of D and C for various temperatures

	297° K.*	353° K.	413° K.
D cm.²/μs	·118 ± ·002	·136 ± ·003	·160 ± ·003
C cm.⁴/μs	·385 ± ·008	·75 ± ·02	1·24 ± ·03

* The constants at this temperature were taken from reference (1).

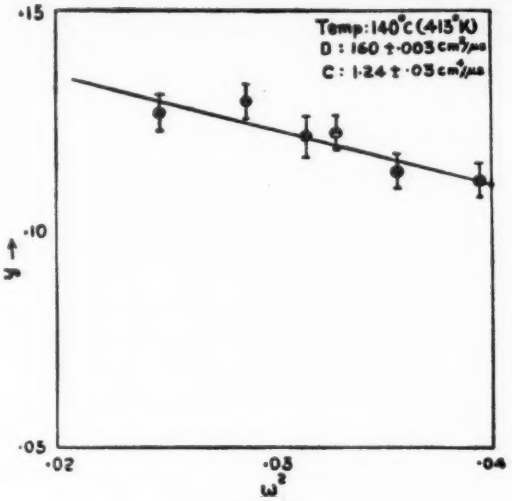

FIG. 2.

TABLE II

Values of β^{-1} in μs for various sizes and temperatures

	297° K.	353° K.	413° K.
Infinite	165±10	244±15	291±17
40×40×40 cm.³ ..	150±8	206±14	231±16
20×20×20 cm.³ ..	119±6	146±10	149±10

DETERMINATION OF β^{-1} BY TRANSMISSION

Since the variation of β^{-1} with temperature by the method described above depends on the value of 'C' at room temperature a direct determination of β^{-1} by a transmission experiment was made. This can be done by observing the time distribution of neutrons from the assembly before and after transmission through a $1/v$ absorber. If n_2 and n_1 are the number of counts at any time, with and without the absorber, as detected by a thick LiI crystal, it can be shown that

$$\frac{n_2}{n_1} = \frac{\int_0^\infty v^3 \exp\left[-\left(\frac{v}{v_0}\right)^2\right] \exp\left[-\frac{a}{v}\right] dv}{\int_0^\infty v^3 \exp\left[-\left(\frac{v}{v_0}\right)^2\right] dv} \qquad (5)$$

where

$$a = \Sigma(a)\, vt$$

$\Sigma(a)$ is the macroscopic absorption cross-section for neutrons of velocity v,

t is the thickness of the absorber,

v_0 is the most probable velocity of neutrons at any given time.

A silver foil of thickness $0{\cdot}1178 \pm 0{\cdot}0004$ cm. was used as the absorber. Corrections were made for the scattering of neutrons by the foil and the angular distribution of neutrons emerging from the assembly. The transmission as a function of the neutron temperature was calculated using the expansion given by Zahn.[3] β^{-1} can now be calculated from the relation,

$$T - T_P = Ae^{-\beta t}$$

where T is the instantaneous neutron temperature and T_P is the equilibrium temperature. The experimental points were fitted to this relation by the method of moments and the values of β and T_P were obtained. The value of T_P was found to be consistent with value of C at room temperature and it was also verified that in the transmission experiment, the neutron temperature approached this value.

The experiment was conducted for a size of $40 \times 40 \times 20$ cm.^{3} at room temperature and the variation of neutron temperature with time in the region

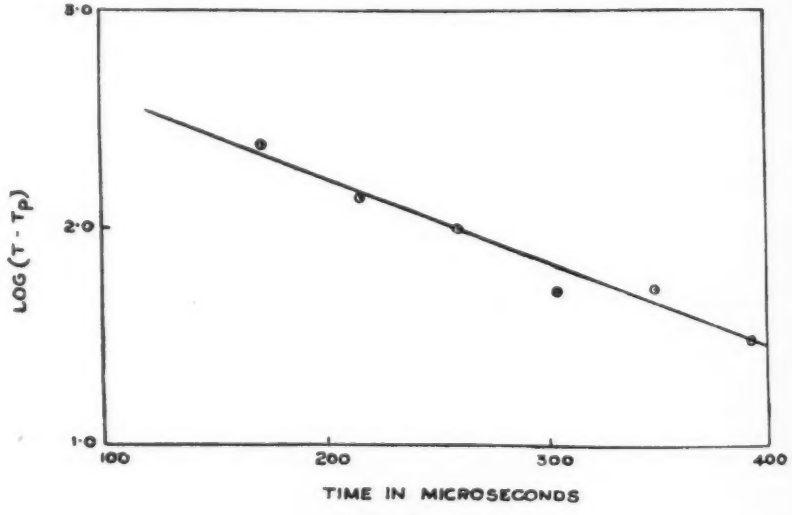

FIG. 3.

from 150 μs to 500 μs was determined. Fig. 3 gives the plot of log $(T - T_P)$ against t. It can be seen that β^{-1} is about 140 μs. This is in excellent agreement with the value of 132 μs calculated from the value of C at room temperature for this size of the assembly.

Discussion

Since $D = \lambda_t v/3$ any variation of $D(T_0)/T_0^{\frac{1}{2}}$ with temperature would be due only to change in the transport cross-section with energy. From Table I it is seen that the maximum variation of λ_t in the range of temperatures between 297° K. and 413° K. is of the order of $(15 \pm 10)\%$.

In Fig. 4 the equilibrium temperature T_P is given as a function of ω^2, for different moderator temperatures. It is seen that for large sizes the equilibrium temperature increases with the increase of moderator temperature while for small sizes it decreases with increase of moderator temperature. This is due to the fact that in small sizes a large portion of

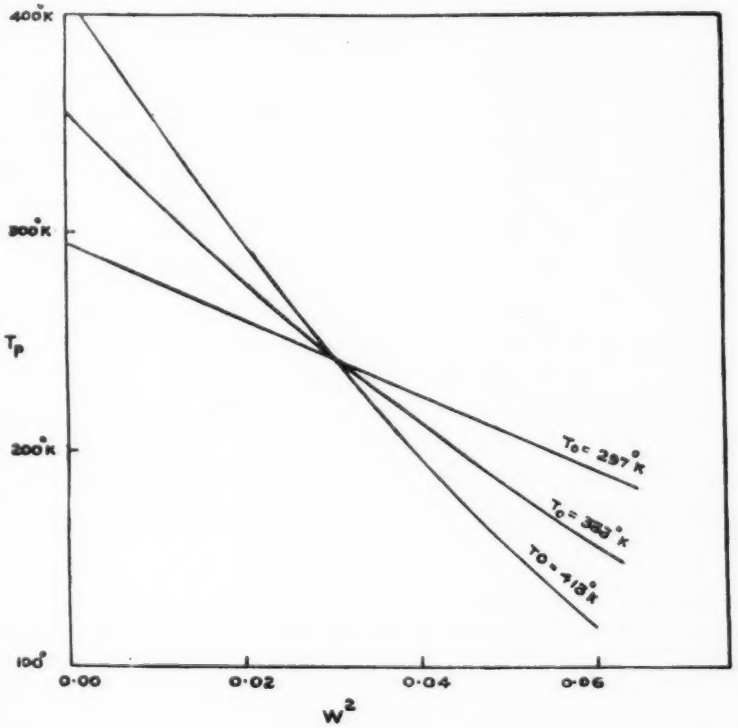

Fig. 4.

the energy is carried away by the escaping neutrons and is not compensated at higher moderator temperatures by the energy transfer from the moderator atom .

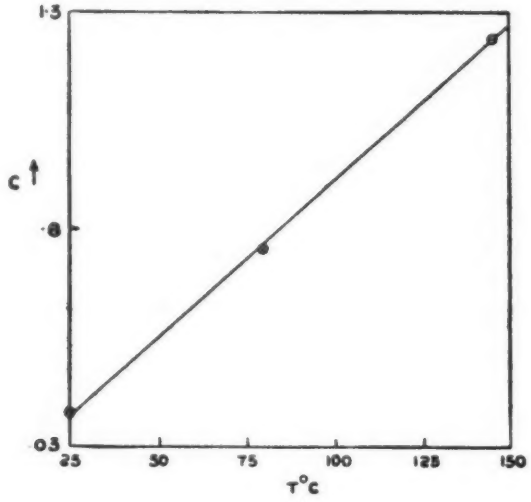

FIG. 5.

From Fig. 5 it is seen that C varies with temperature approximately as

$$C(T_0) = 0{\cdot}007\, T_0 - 1{\cdot}8.$$

This shows that within the range of temperature used, the relaxation time β^{-1} increases with temperature, or in other words, γ, the heat transfer coefficient, decreases with the increase of moderator temperature. This result seems to be in contradiction with the conclusions derived from the Debye model.[2]

Our thanks are due to Mr. M. P. Navalkar, Mr. F. R. Bhathena and to Mr. S. K. Ambardakar for their help in conducting the experiment.

REFERENCES

1. Iyengar, S. B. D., Mani, G. S., Ramanna, R. and Umakanth, N. — "Slowing down and diffusion of neutrons in BeO," *Proc. Ind. Acad. Sci.*, 1957, **45**, 215.
2. Von Dardel .. "The interactions of neutrons with matter studied with a pulsed neutron source," *Thesis* (Goteberg), p. 73.
3. Zahn .. *Phy. Rev.*, 1937, **52**, 67.

THE INPUT AND OUTPUT SYSTEM OF THE T.I.F.R. COMPUTER

By B. K. Basu and K. Bakhru

(Tata Institute of Fundamental Research, Bombay)

Received January 10, 1957

(Communicated by Prof. Bernard Peters)

Abstract

This paper describes the logical circuits which have been incorporated in the Input-Outpur unit of a pilot electronic digital computer. The unit is used to feed the input data into the calculator from a punched tape through a Photo-electric tape reader and to print out the results, after computation, by standard teletype equipment.

Introduction

The Input-Output unit of the Pilot Digital Computer which has been developed in the Tata Institute of Fundamental Research, consists of a Ferranti-Photo-electric tape reader for transferring the data to the machine, an Olivetti page printer and a reperforator for printing out the results of the calculations and preparing the tape respectively. The photo-electric tape reader is used to transfer information in parallel from a standard five hole tele-type tape into the calculator. Four of these hole positions represent a binary coded decimal number. The fifth hole when present inhibits the transfer of information contained in that row of the tape to which it belongs. The tape reader is connected to the four least significant digits of a shift register called the multiplier-quotient register (M.Q. Register). The process of reading consists of shifting the contents of M.Q. register four places to the left and writing into it the contents of a row from the paper tape. The input order is of the form I (n), where the address part (n) dictates the number of shifts to occur in the process. In other words, $n/4$ gives, to the nearest higher integer, the number of rows in the tape to be read consecutively in one operation.

Since the tape reader is directly associated with one of the registers of the Arithmetic unit of the machine (M.Q. Register), the machine is tied up until the whole input order has been executed. This is avoided in the output order by providing an auxiliary output register and an output control. On receiving the output order the internal control of the machine delivers the 5 bit output information to the output register and enables the machine

to go ahead with further calculations. However, in the case of two successive output orders the logic of the unit requires the machine to wait until the execution of the first order is complete. The content of the output register is then serially shifted out to the perforator and/or page printer by thyratron pulses, generated from the 50 cycle a.c. mains.

THE INPUT UNIT

The input tape consists of a set of five digit positions each of which when perforated represents a 1 and otherwise a 0. This set of holes punched in a row across the tape constitutes a character which is a binary coded decimal digit. In addition to these holes there is a sprocket hole punched in the centre of the tape. This hole is smaller in dimension than the others and is always present in a row irrespective of others. For feeding a problem to the calculator the tape is perforated, properly by a separate tape perforator and then used with the tape reader.

The photo-electric tape reader, as the name implies, has photo-cells for sensing the punched tape and a differential gear arrangement for moving the tape. The differential gear rotates continuously with the help of a motor. On either side of this gear, on a common shaft, are coupled to it two drums called the ' Brake drum ' and the ' Clutch drum ', either of which can be stopped with the help of a pair of brake systems operated by electromagnets. If one of the drums is stopped the other rotates with double the speed. The tape is pressed close to the brake drum and moves due to friction when the latter rotates.

The sensing photo-cells along with some associated circuits are mounted inside a closed chamber. Each photo-cell senses only holes pertaining to a particular column in the tape. At the top of the chamber, across the path along which the tape moves, there are 8 holes in a row. These holes have the same dimensions as the perforations on the tape. Six out of the eight holes are utilised to read the five hole tape-one for each digit hole of the tape, and one for the sprocket hole. The hole corresponding to the sprocket hole is similarly placed in the row as the latter. The photo-cell corresponding to the sprocket hole is called the ' Location Photo-cell '. As the tape moves over these holes, light falls intermittently on the photo-cells through the holes in the tape. This causes the digit photo-cell outputs to become positive for the time during which light falls on them. The output of the location-photo-cell is, however, a negative square wave which starts later than the digit photo-cell outputs, because of the smaller dimensions of the sprocket hole in the tape.

The circuitry which has been built to utilise the tape reader, consists of (1) the necessary controls for the motion of the tape, (2) amplifiers for amplifying the output of the photo-electric cells, and (3) the gating system for transferring the data from the tape to the machine. In the following section the parts played by these circuits are described with the help of logical diagrams.

When the internal control of the calculator receives an input order, the tape is allowed to move to the next row of holes to be sensed by the photo-electric cells. Simultaneously the M.Q. register is shifted 4 places to the left, so that the 4 least significant bit positions of this register are cleared. In this position the M.Q. register is ready to receive fresh information from the tape reader.

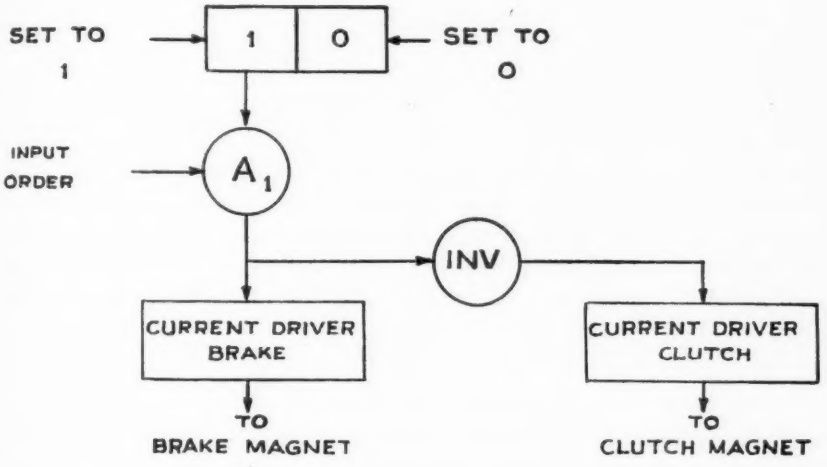

FIG. 1. Logical Circuit Diagram for controlling the motion of the tape.

Fig. 1 shows the logical circuit diagram for controlling the motion of the tape. The input flip-flop, which is set to the state '1' by the internal control of the computer in one of its micro-operations, produces a negative signal as one input to the 'And' gate A_1, which is a negative 'And' gate. The presence of an input order provides another negative signal as the second input to the 'And' gate A_1. When both the input signals to the 'And' gate A_1 are negative, the resultant output from it, which is also negative is fed to the current driver of the brake-electro-magnet. The current through this magnet is cut off, releasing the brakedrum. The output of the 'And'

gate A_1 is simultaneously fed, after inversion, to the current driver of the clutch electromagnet, thus engaging the clutch and allowing the tape to move.

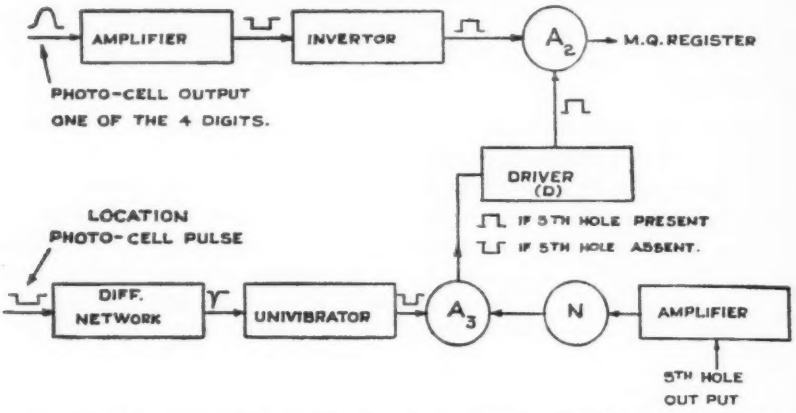

FIG. 2. Block diagram of the gating system for transferring the data from the photo-cell reader to the machine. Only one of the four photo-cell outputs is shown.

In Fig. 2 is given the block diagram of the gating system, which transfers the information from the reader to the M.Q. register. When a row of holes, forming a character is sensed by the reader, the signals from the photo-cells are applied to the corresponding amplifiers. The amplifiers, which are D.C. coupled, amplify the pulses and shape them so that the outputs from them are in the form of positive square waves. These square waves are applied to the respective ' And ' gates A_2.

The signal from the location photo-cell which is a negative pulse of square wave form is differentiated. The pulse obtained at the leading edge is utilised to trigger a univibrator, which gives a negative square pulse of known width as its output. This output is given to another ' And ' gate A_3. The second input to the ' And ' gate A_3 is the signal from the 5th hole, after proper amplification, through the ' Not ' gate N. The output of the ' Not ' gate N is a negative square signal if the 5th hole is absent, and a positive signal of the same shape if the 5th hole is present.

Normally when a character is to be read, the output of the ' And ' gate A_3 is a negative pulse which is fed to the driver D which in its turn opens the ' And ' gate A_2, so that the information is gated down to the M.Q. register. On the contrary, if any particular character in the tape is to be discarded, the 5th hole in the same row is punched. Then, the presence of the 5th hole

positive signal at the ' And ' gate A_3 presents no output signal from that gate and hence the gate A_2 fails to convey the information to the M.Q. register.

When the last character of the tape as set by the address part (n) of the input order I (n) has been sensed by the reader, the internal control of the calculator sets the input flip-flop to the state ' 0 ', so that current passes through the brake magnet, while no current passes through the clutch magnet. Thus the tape is stopped. Arrangements have been made inside the computer with the help of the location photo-cell signal, so that the tape is halted only when a character is in the read position. The location photo-cell pulse has further been utilised for safe operation of the gating system, by feeding it through ' Not ' gate to the shifting cycle of the internal control, so that the shifting of the 4 bits in the M.Q. register does not take place till the gating pulse from the driver D has died down.

It is to be noted that all the circuit elements in the unit are D.C. coupled, except for the location photo-cell circuit which contains the univibrator. The univibrator serves a two-fold purpose, (1) It keeps the width of the location photo-cell pulse at the input of the ' And ' gate A_3 within limits so that proper inhibition by the 5th hole takes place, (2) Although the tape stops when the holes in the last character of the previous input order are in the read position, the next input order cannot read this character for the second time, because only the leading edge of the location photo-cell can trigger the univibrator.

The Output Unit

The tele-type writer and the Page Printer which are used to print out the results from the calculator utilise a 5 unit code. Each unit of the code requires a signal lasting for 20 millisecond. Each train of these pulses is to be preceded by a start pulse which sets the printing mechanism into operation and is followed by a stop pulse, which stops the printer, thus making a total number of seven pulses to be fed to the printing mechanism.

Since the calculator as a whole works in the parallel mode, while the printing mechanism requires a train of 7 pulses to be fed serially for printing out a character, an intermediate stage is necessitated to change from the parallel to the serial system. Further, since the printing unit is a purely mechanical system, it works at a speed which is much slower than the internal speed of the machine. Therefore, it is advantageous to work out a design for the output unit which will allow the machine to go on with further calculations while the output order is being executed.

The first of these requirements has been fulfilled by incorporating in the unit an auxiliary register known as the output register, while the second requirement has been partly met with the design of the output drivers. The logical circuitry which has been described below consists of two parts: (1) the output register, and (2) the output or the gate drivers. When the output order is sensed by the output control of the computer, it transfers the number from the M.Q. register to the output register and signals the internal control of the machine to go ahead with the next order. The contents of the output register are then serially sent to the printer by a shifting process, carried out by the output drivers.

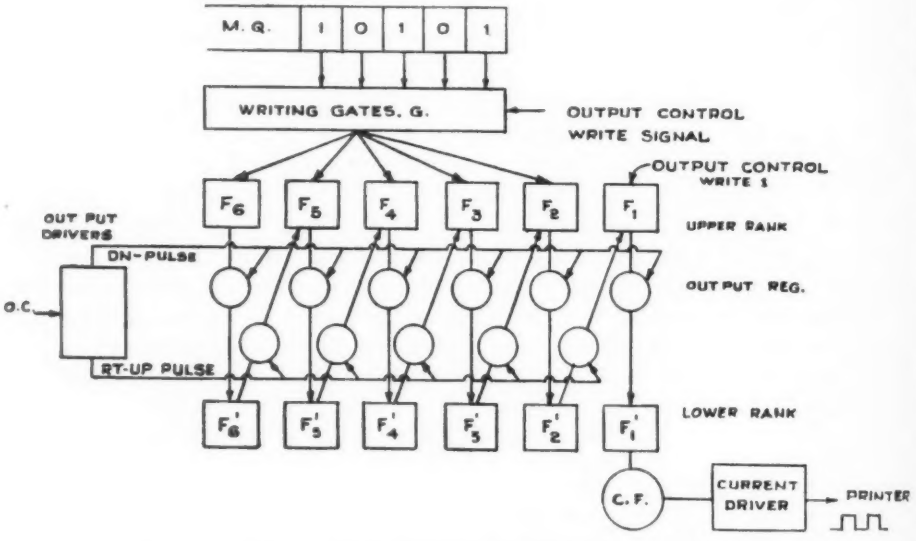

FIG. 3. Block diagram of the output register showing the shifting process.

Fig. 3 shows the block diagram of the output register with the shifting facilities that have been built in. The output register is a double rank register consisting of six identical stages. In each stage there is one upper rank flip-flop F (F_1, F_2,.....F_6) and a corresponding lower rank flip-flop F′ (F_1', F_2',.....F_6'). The upper rank register (U.R.) acts as a buffer register (temporary storage space) to facilitate serial shifting out of the contents of the lower rank register (L.R.) To achieve a right shift of the L.R. the contents of L.R. is first gated up one place to the right (*i.e.*, F_6' to F_5, F_5' to F_4, etc.) and then gated vertically down (*i.e.*, F_6 to F_6', F_5 to F_5', etc.).

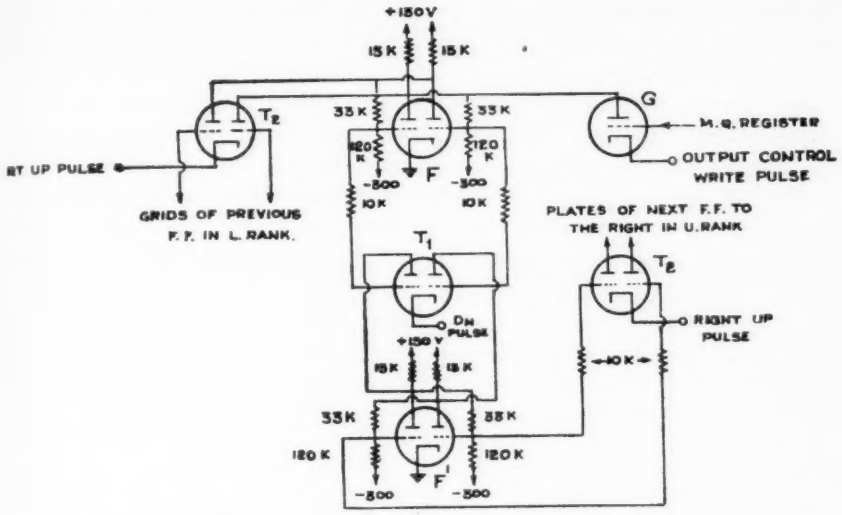

FIG. 4. Circuit diagram of one of the units of the output register.

Fig. 4 shows one stage of the output register with the required gating circuitry. Double triodes T_1 and T_2 form the gate tubes to effect vertical down and right-up shifts respectively. All T_1 cathodes are connected to the gate down driver and the T_2 cathodes to the gate right-up driver. Gating is done by lowering the cathode voltage of the gate tube in which one of the two sections of the tube conducts. This type of double gating has been used to make transfer to F or F′ independent of their previous states. This is necessitated by the wave-form requirements of the signal which is fed to the printer from F_1' in the lower rank. For gating down the information from M.Q. register to the output register another set of gates is employed denoted in the figure by G.

To start with, the upper rank of the output register is cleared in the first micro-operation of the output control. In the next operation, the number is gated down from the 5 most significant bit positions of the M.Q. register to the last 5 flip-flops in the upper rank of the output register. The first flip-flop is set to state ' 1 ' and this acts as a start signal. The output drivers have been so designed that the shifting operation begins always with the down pulse coming first. This transfers the contents of the U.R. to the corresponding flip-flops in the L.R. The first flip-flop of the L.R. (F'_1) is connected through a cathode follower to a driver which drives current through the magnetic circuit of the printer. Ten milliseconds after the

occurrence of the first down pulse, a right-up pulse shifts the contents of the lower rank to the upper rank but one place to the right and writes a zero in the last flip-flop F_6 of the U.R. The right-up pulse is followed by a down pulse after another 10 milliseconds. The contents of the U.R. are once again shifted down, sending the first bit brought from the M.Q. register to the printer, 20 milliseconds after the start signal. The process is repeated till all the 7 pulses required for printing a character are shifted out to the printer.

The gate pulses are obtained from the cathode of two thyratrons which have been synchronised with the mains frequency by connecting their grids in push pull to a small a.c. voltage derived from a.c. mains. Advantage has thus been taken of the a.c. mains frequency in firing the two thyratrons alternately so as to get two sets of pulses, one from each thyratron, separated by 20 milliseconds, but one set lagging behind the other by half a cycle.

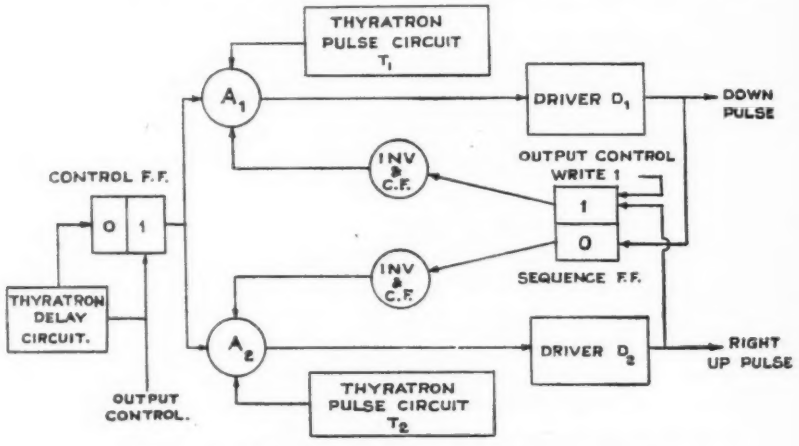

FIG. 5. Logical circuit diagram of the output drivers.

The logical diagram shown in Fig. 5 gives the shift pulses in the correct sequence. T_1 and T_2 are the two thyratron pulse generating circuits. F_1 is the sequencing flip-flop which changes its state alternately with each driver output pulse, the down pulse setting it to the state '0' and the right-up pulse to '1'. F_2, called the control flip-flop, starts the shifting operation when it is set to the state '1' by the output control. Once the control flip-flop is set to the state '1', it carries out the shifting process to the end by opening up the gates A_1 and A_2 alternately. This allows the internal control of the machine to proceed with further calculations, except

in the case when two output orders occur consecutively. The control has then to wait till the shifting operation for the first output order is complete.

The output control in one of its minor operations sets the sequencing flip-flop to the state ' 1 ', and this is responsible for the down pulse coming first. Subsequently in another operation it sets the control flip-flop also to the state ' 1 '. The gate A_1 is now open and the first pulse from the thyratron T_1 is gated out. This is used as the down pulse through the driver D_1. The output of the driver D_1 sets the sequencing flip-flop F_1 to the state ' 0 ', so that the gate A_1 is closed while the gate A_2 opens the control flip-flop remaining in the state ' 1 '. Now the pulse from the thyratron T_2 is gated out and through driver D_2 causes the right-up pulse. The output of the driver D_2 sets the sequencing flip-flop to the state ' 1 ', so that the cycle repeats itself. At the start of the shifting cycle, when the output control sets the control flip-flop to the state ' 1 ', it simultaneously sets also a thyratron delay circuit into operation which gives a pulse after a delay of 140 milliseconds (time taken by the output signal chain). This pulse is utilised to get the control flip-flop to the state ' 0 ', so that the shifting process stops. The setting of the control flip-flop to state ' 0 ' also makes the output control ready to receive the next output order.

Working Experience

The input sequence could not be tested out fully for reliability as some parts of the input tape reader were broken during shipment. Because of the limited workshop facilities, the repair could only bring it upto the standard just sufficient to test the input system. However, for the machine, alternate manual means have been provided for feeding the input data.

The output mechanism is working with the computer ever since the machine has been put on. Except for one or two valve failures no other faults occurred.

Acknowledgment

The authors wish to express their appreciation to Dr. D. Y. Phadke for initiating the work reported in this paper. Thanks are due to Messrs. M. M. Farooqui, S. P. Srivastava and B. B. Kalia for their ungrudging help.

A TWO DIMENSIONAL FERRITE-CORE MEMORY

By M. M. Farooqui, S. P. Srivastava and R. N. Neogi
(Tata Institute of Fundamental Research, Bombay)

Received January 10, 1957
(Communicated by Prof. Bernard Peters)

Abstract

This paper describes a two dimensional matrix memory using ferrite-cores. A unit consisting of 100 words of 11 binary digits each has been constructed for parallel operation. The word drive is from a biased switch-core matrix, while the digit drive makes use of pulse—transformers. Logic and circuit techniques enable high discrimination between wanted and unwanted signals.

A semi-automatic method for testing the memory cores is also described.

Introduction

The potentiality of magnetic ferrite-cores with a rectangular hysteresis loop as binary storage elements for digital computer was realised earlier by Forrester.[1] Later, Papian[2,3] and almost simultaneously Rajchman[4,5] showed the practicability of such a system by successfully operating memories of fairly large capacity. This paper describes a modest attempt in this direction. A memory of 100 words, 11 bits each, has been constructed to operate with a small digital computer at the Tata Institute of Fundamental Research, Bombay.

The Principle of Operation of the Memory

The two stable states required for storing binary information in magnetic cores are the states of positive and negative magnetisation. These are the states corresponding to the position A_0 and A_1 on the hysteresis loop and can be termed as the 0- and the 1-states respectively (Fig. 2). Consider a number of such cores with an ideally rectangular hysteresis characteristic, arranged in rows and columns in the form of a matrix. Each core in the matrix is linked by three wires—a row wire, a column wire and an output wire linking through all the cores in a row of the matrix. Suppose I is the minimum magnitude of the current required to magnetise the cores to saturation. Any core within the array can then be magnetised to the 1-state or the 0-state by sending current pulses of magnitude $-I/2$ or $+I/2$,

respectively, through the appropriate row wire and the column wire simultaneously. The condition of the other cores in the array is, however, not disturbed by this method of writing, because they receive either half the critical current excitation or no excitation at all.

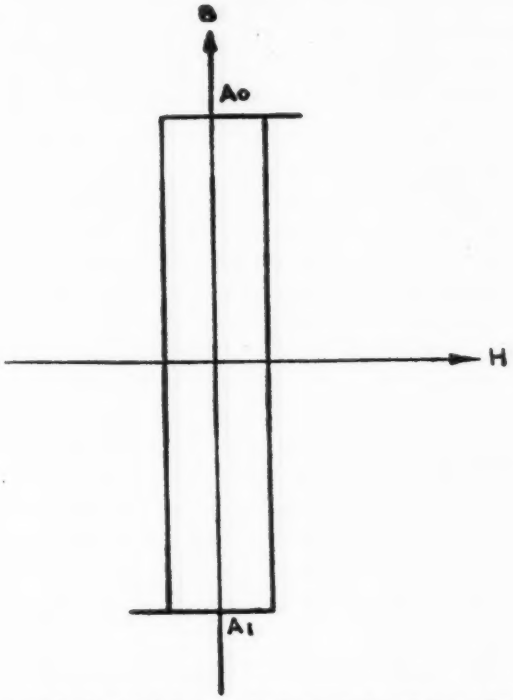

FIG. 2. Ideal rectangular hysteresis loop for ferrite-cores. A_0 and A_1 are the two stable states.

To regain the stored information, the method of reading adopted is to send always a current pulse of magnitude I/2 and of one polarity, say + I/2, through the row wire and the column wire simultaneously. It can be easily verified that the selected core, only if originally in the 1-state, will give an output because of the change of flux associated with the transition from the 1- to the 0-state. This process of reading out destroys the stored information (*i.e.*, leaves the element in the 0-state); hence it is necessary after each read cycle to rewrite the information that has been read out. This is accomplished by applying a current pulse equal to − I/2 simultaneously to the row and the column of the matrix if a 1 has been read out.

Deviation from the ideal rectangularity of the hysteresis characteristic will have two effects on the reading out of imformation. Firstly, there will be a small signal due to the read out of 0. Secondly, there will be a contribution to the signal from the half excited cores (I/2 excitation). For a large array the cumulative effect of the latter will tend to decrease considerably the ratio of the 1 read-out signal to the 0 read-out signal. To minimise this effect the output wire is linked in one sense through half the cores of the array and in the opposite sense through the other half, so that the contribution to the output from the half excited cores becomes zero on the average.

THE 100-WORD 2-DIMENSIONAL MEMORY

The 100-word 11-bit memory is in the form of a 2-dimensional matrix. It is arranged in 100 columns and 11 rows. Each column represents a word and 11 rows represent the 11 digits of a word. The magnetic cores for the matrix have been obtained from the General Ceramic Corporation, U.S.A. They are torroidal cores (F-394) and have the following dimensions: ·080″ O.D., ·050″ I.D. and ·025″ thickness. The construction of the memory matrix is quite simple and straightforward as can be seen from Fig. 3. Each core in the matrix is linked by three wires: the x-wire or the digit-drive wire connects all the cores of the same row; the y-wire or the word-drive wire links all the cores of the same column and the output wire links all the cores of the row. The output wire is turned around twice over the entire length—first in one direction through the cores of alternate columns and then in the reversed direction through the remaining cores.

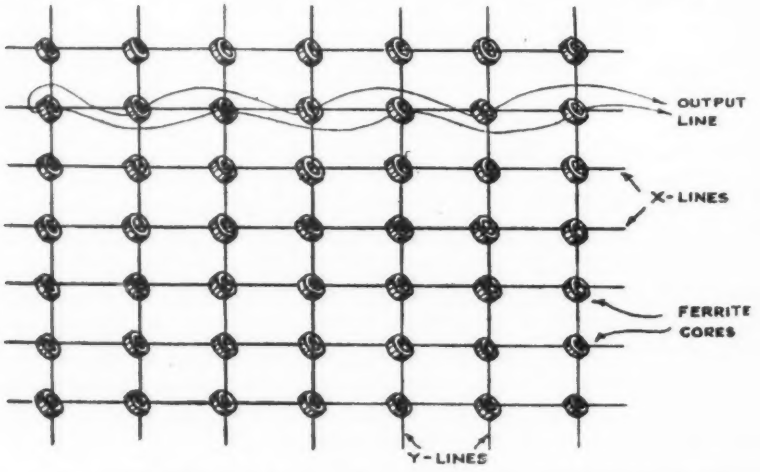

FIG. 3. Threading of wires through the cores in the main memory matrix.

Various current coincidence schemes for reading from and writing in the memory can be worked out. The one that is being used is shown in Fig. 4 in terms of the X- and Y-dirves. Reading or writing is done simultaneously for all the 11 bits constituting a word. The word is selected by a particular Y-drive, while parallel operation of all the bits is achieved by the manipulation of the individual X-drives. One characteristic feature of the coincidence scheme is that the drive–sequence to the memory is the same for reading 0 and writing 0 and also for reading 1 and writing 1.

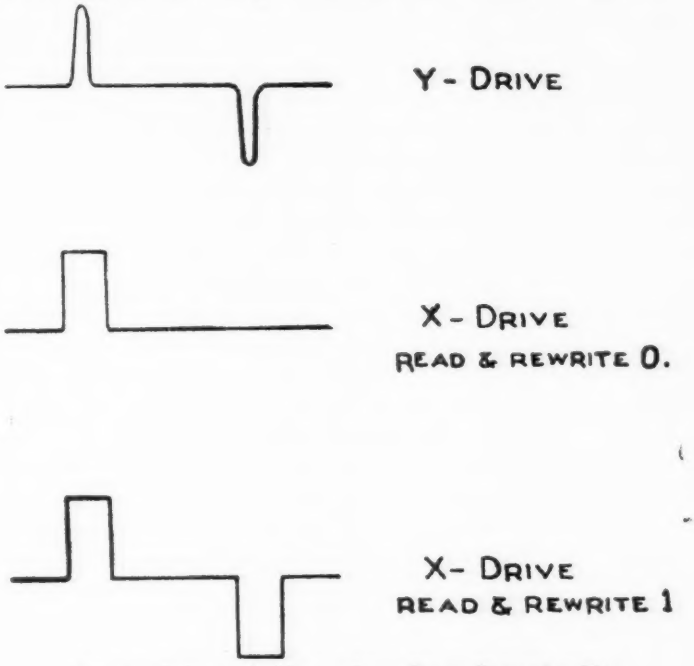

FIG. 4. Current coincidence scheme for reading and writing.

This happens because reading is always followed by re-writing and writing takes place only after erasing the previously stored information. To re-write 1, the memory pulse output is fed back to pass the second pulse in the X-drive sequence. It may be mentioned here that the Y-dirve pulse is made to occur somewhere during the flat portion of the X-drive pulse. This, with the help of strobing, enables a time discrimination between the actual output pulse and the noise created by the rise and fall of the X-drive pulse.

The arrangement of the memory driving system is shown in schematic in Fig. 5. X-drives of both polarity are obtained with the help of pulse

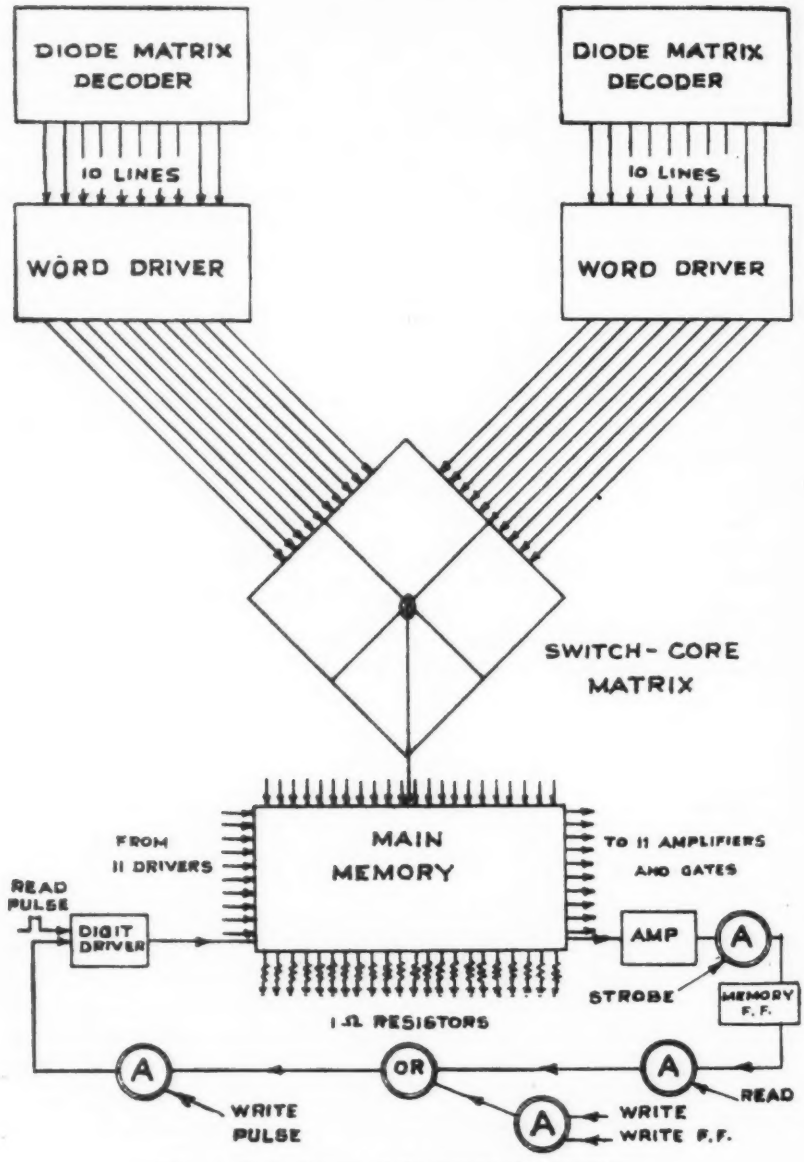

FIG. 5. Block diagram of the memory driving system.

ransformers having two primary windings and one secondary winding. A primary drive of 75 m.a. is required to obtain the required secondary drive of 500 m.a. 500 m.a. is half the current required to flip the memory cores from one state to the other (I/2 mentioned before). The transformers are wound on C-cores obtained from the English Electric Company, London. The primary and secondary turns are respectively 75 and 10.

The same excitation of 500 m.a. is obtained for the word drive (Y-drive) with the help of another 10×10 coincident current core matrix. This is called the switch-core matrix. Each one of this matrix drives one particular column of the main memory. The cores (F-262) used for this matrix are of bigger size (I.D. ·187″, O.D. ·375″ and thickness ·125″) but have the same characteristic as the memory cores. There are four windings linking each core of this matrix—two selection windings X^1 and Y^1, individual output windings and a d.c. bias winding linking in the same sense through all the cores of the matrix. The bias winding, however, opposes the excitations applied to the X^1 and Y^1 windings. D.C. bias is employed only to bring back the selected core to its original state after the excitation. If square current pulses are applied simultaneously to the two selection windings X^1 and Y^1 of any core an output of the form shown in Fig. 4 is obtained, as the Y-drive pulse for the memory matrix. This output consists of two pulses one at the leading edge and the other at the falling edge of the original current pulse. The pulse at the falling edge occurs because of the constant direct current bringing the switch cores to the original biased condition. The ten X^1 and ten Y^1 windings have 15 turns each. Each turn of these windings links every core along the respective co-ordinates. The output winding consists of just a single turn. The d.c. bias winding of 10 turns threads through each core, carrying a current of 100 m.a. With such an arrangement the ratio of the output of the selected core (the core for which both X^1 and Y^1 drives are present) to that of the half-excited core (the core for which either of the X^1 or Y^1 is present) is found to be more than 8 : 1.

The excitations for the X^1 and Y^1 selection windings of the switch-core matrix are obtained from two identical constant current drivers. Their operation can be understood by referring to Fig. 6 (*a*), where the circuit for one of the drivers is shown. The diode matrix decoder supplies + 100 volts at the selected terminal and + 60 volts at the non-selected terminals. These potentials are fed through a cathode follower to the grids of the driver valves V_3. All the driver cathodes are joined together and kept at + 130 volts by a feedback stabilised system controlled by the cathode follower V_2, V_1 (Fig. 6*a*) and the amplifier inverter V_4. All the driver valves are

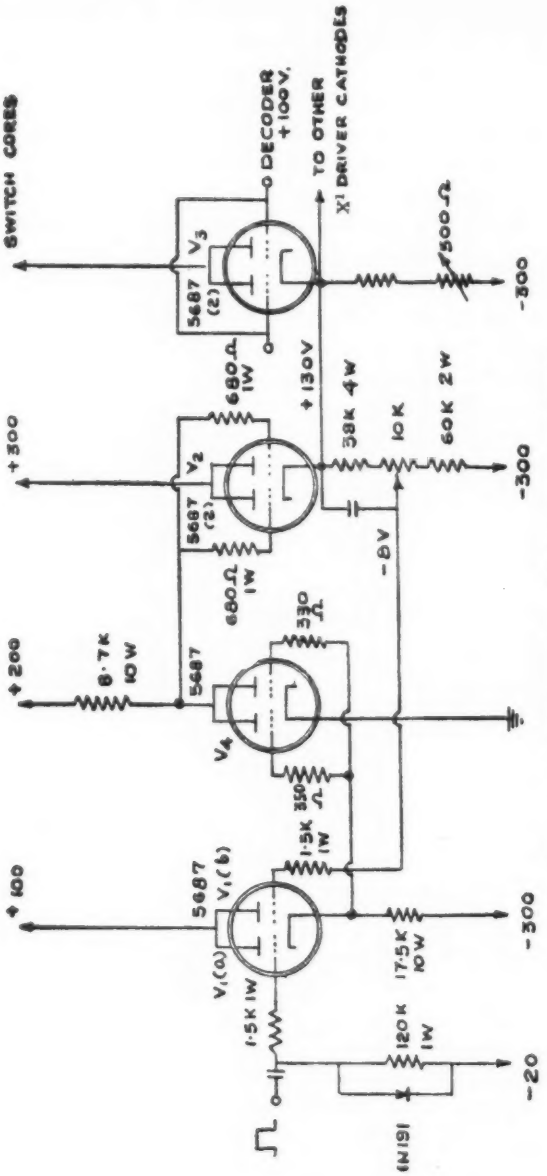

FIG. 6. (*a*) Arrangement for driving switch core-matrix.

therefore normally cut off and current slightly more than the driving current required flows through the valve V_2. The excitation pulse of about 30 volts is given to the normally cut-off tube V_1 (*a*). This pulls down the grid of V_2 to 60 volts. The cathode of V_2 is, however, arrested by the selected driver valve V_3. V_2 thus gets cut off and the driving current flows through V_3. The magnitude of the driving current is determined mainly by the grid potential of V_3 (100 volts), the variable cathode resistance RK (3 K – 3·5 K) and the cathode return potential (— 300 volts). The cathode return potential is intentionally made low (— 300 volts) to make the current drive somewhat independent of the variation in the driving tube characteristics.

In Fig. 6 (*b*) is shown the circuitry used to obtain the digit drives for the memory matrix. A positive pulse at the grids of the driver V_x, normally biased to cut off, supplies the required X-drive excitation to the memory cores. Although drivers identical to the ones used with the switch-core matrix could also have been employed for the digit drives, the present method was settled on to reduce the overall current comsumption. However, it must be pointed out here that in practice it has been found necessary to adjust the X-drives periodically for proper functioning of the memory.

Figure 7 shows the memory outputs obtained with the driving systems employed. The ratio of the wanted to the unwanted signal in the worst case is more than 4 : 1. It has, therefore, been found adequate to use strobing after linear amplification rather than resort to the complicated integration techniques usually suggested in the literature.

The memory output is of both polarity because of the way the output winding is threaded, through the cores. This method of winding is found necessary to get the cancellation of the contributions to the output from the half-excited cores. The memory output is made unidirectional by passing the output signal through a pulse transformer and a full wave diode rectifier system. The unidirectional output thus obtained is fed to the output amplifier. The output amplifier (Fig. 8), consists of a two stage a.c. coupled amplifier and a cathode follower. It amplifies the ·15 volts input signal to 50 volts. The cathode follower output obtained is fed to the suppressor of the gating tube 6AS6, the strobing pulse of 1 μ sec. duration is applied to its control grid. The strobbed output is finally fed to flip-flop for controlling the rewrite.

Improvement in Logic

One of the main disadvantages in using the switch cores as drivers is that the magnitude of the driving current is found to depend quite appreciably on the presence or absence of the second pulse on digit drive line. As

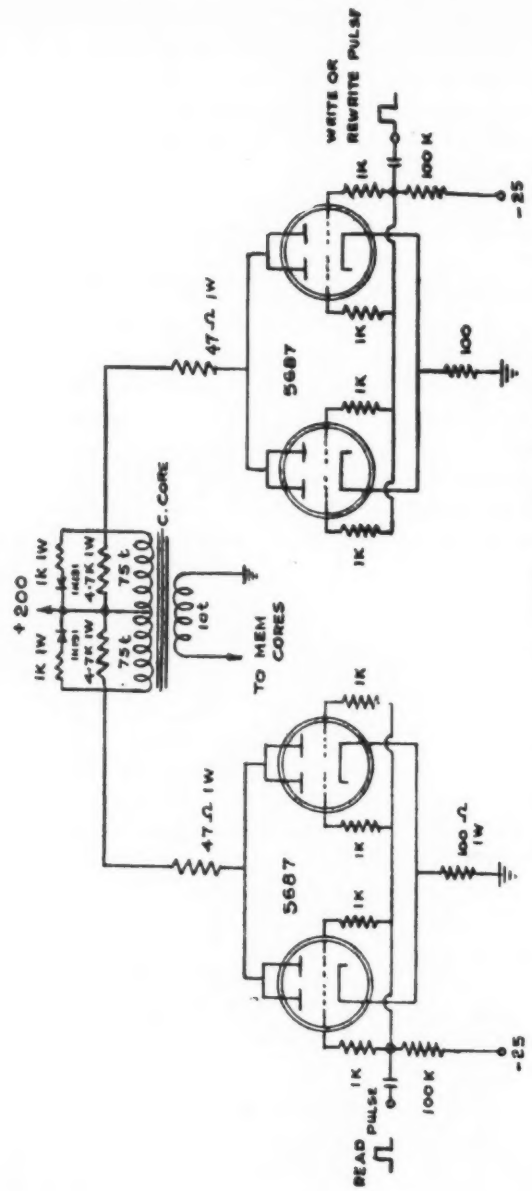

FIG. 6. (*b*) Row (Digit) drivers for the main memory.

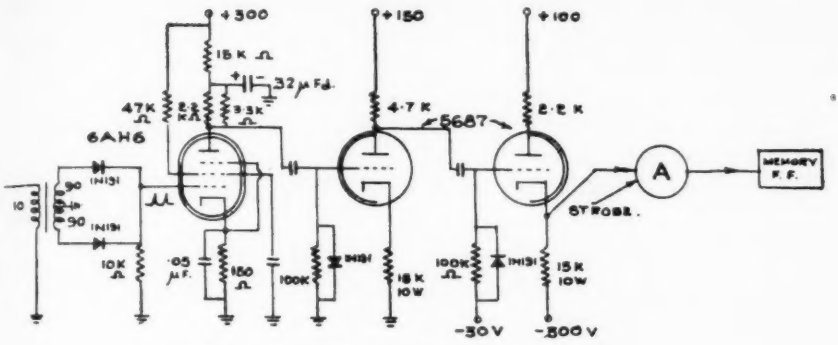

FIG. 8. Memory output amplifier. Gain—330.

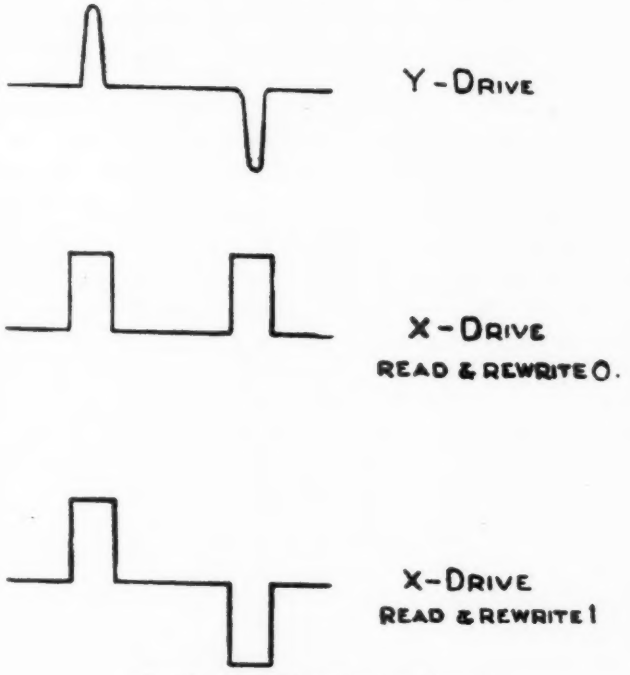

FIG. 9. Modified read–write scheme.

observed across a 1 ohm terminating resistance the Y-drive is minimum when the rewrite pulse is present in all the rows. Therefore, the setting of the Y-drive becomes somewhat critical. One way of avoiding such variations is to increase the terminating resistance and also to increase the Y-drive.

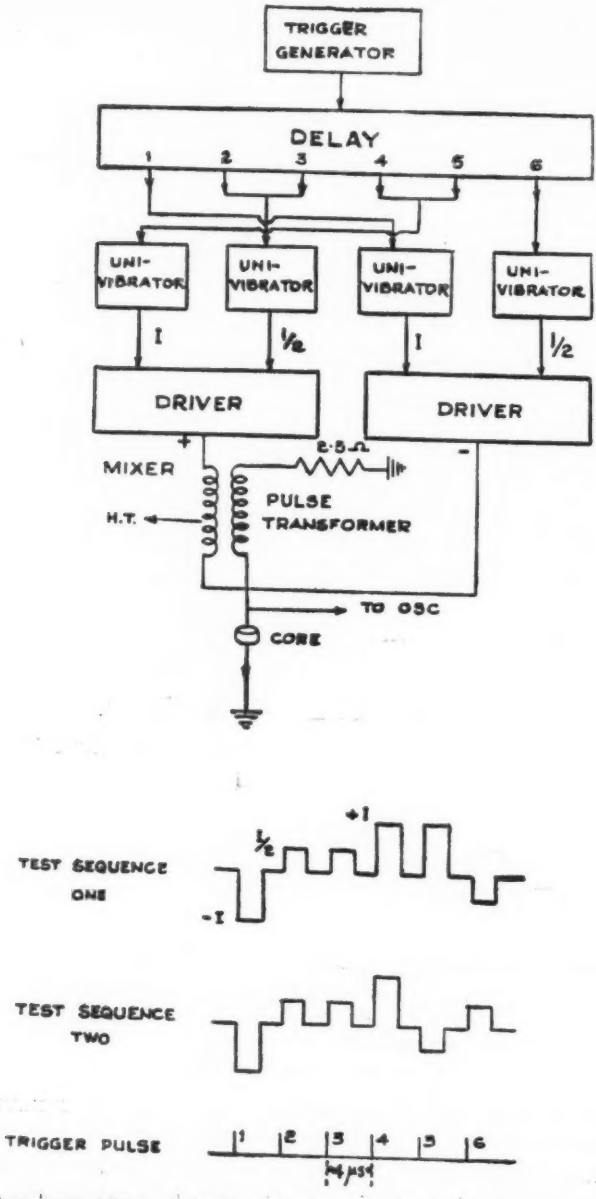

FIG. 10. Arrangement for rapid testing of ferrite-cores. Two test sequences used are shown.

But this distorts the shape of the driving pulse. The other way of attacking the problem would be to construct a logic, if possible, which will overcome the effect of this variation. Investigation along the second line has given rise to a read-write logic (Fig. 9) slightly different from the original one. The Y-drive should be adjusted to be 500 m.a. under the worst condition. One can easily visualise that due to the positive action involved in writing a 0, the possibility of writing a 1 in place of a 0 and *vice-versa* will be minimised.

Method of Rapid Testing of the Cores

Because of the elaborate structural feature of the storage unit, it is very troublesome to replace cores once they have been wired in position. It is e sential therefore to pre-test each single core thoroughly and to make sure that only cores with satisfactory magnetic characteristics are used as the matrix elements. A semi-automatic method has been developed to test the cores in rapid succession. With the help of this method cores have been tested at the rate of approximately 200 per hour. Fig. 10 shows in schematic the experimental arrangement for testing the cores and also the two test sequences of pulses that were used. As can be seen the principal contributing factor to speed up testing is the use of a single wire for reading as well as writing.

The cores were tested with specific reference to three principal features: the amplitude of the wanted signal, the ratio of the wanted to the unwanted signal, and the asymptotic behaviour of the core under a set of half excitations. For observing the third phenomenon the excitation pulse chain used, though small in length, was found quite adequate for the purpose of selection. This has been borne out amply by the actual behaviour of the selected cores in the memory unit now operating as part of the pilot digital calculating machine.

Conclusion

From the satisfactory operation of the present memory system one can conclude that it will be possible to construct a memory of much larger size than the present one. Meanwhile, to evaluate the merits of different systems a three dimensional memory of 256 words 12 bit each has been constructed. It is being tested now employing the logic used by Papian.[2,3]

Acknowledgment

The authors are thankful to Dr. D. Y. Phadke for many helpful suggestions. Thanks are also due to Dr. R. Narasimhan, Mr. B. K. Basu and Mr. M. M. Dosabhai, for their untiring help.

REFERENCES

1. Forrester, J. W. .. "Digital Information Storage in Three Dimensions using Magnetic Cores," *Jour. Appl. Phys.*, Jan. 1951, **22,** 44.
2. Papian, W. N. .. "A Coincident-current Magnetic Memory Cell for the storage of Digital Information," *Proc. I.R.E.*, April 1952, **40,** 475.
3. ———— .. "New Ferrite-core Memory uses Pulse Transformers," *Electronics*, March 1955, **28,** 194.
4. Jan Rajchman .. "Static Magnetic Matrix Memory and Switching Circuits," *R.C.A. Review XIII*, June 1952, 183.
5. ———— .. "A Myriabit Magnetic Core Matrix Memory," *Proc. I.R.E.*, October 1953, **41,** 1407.

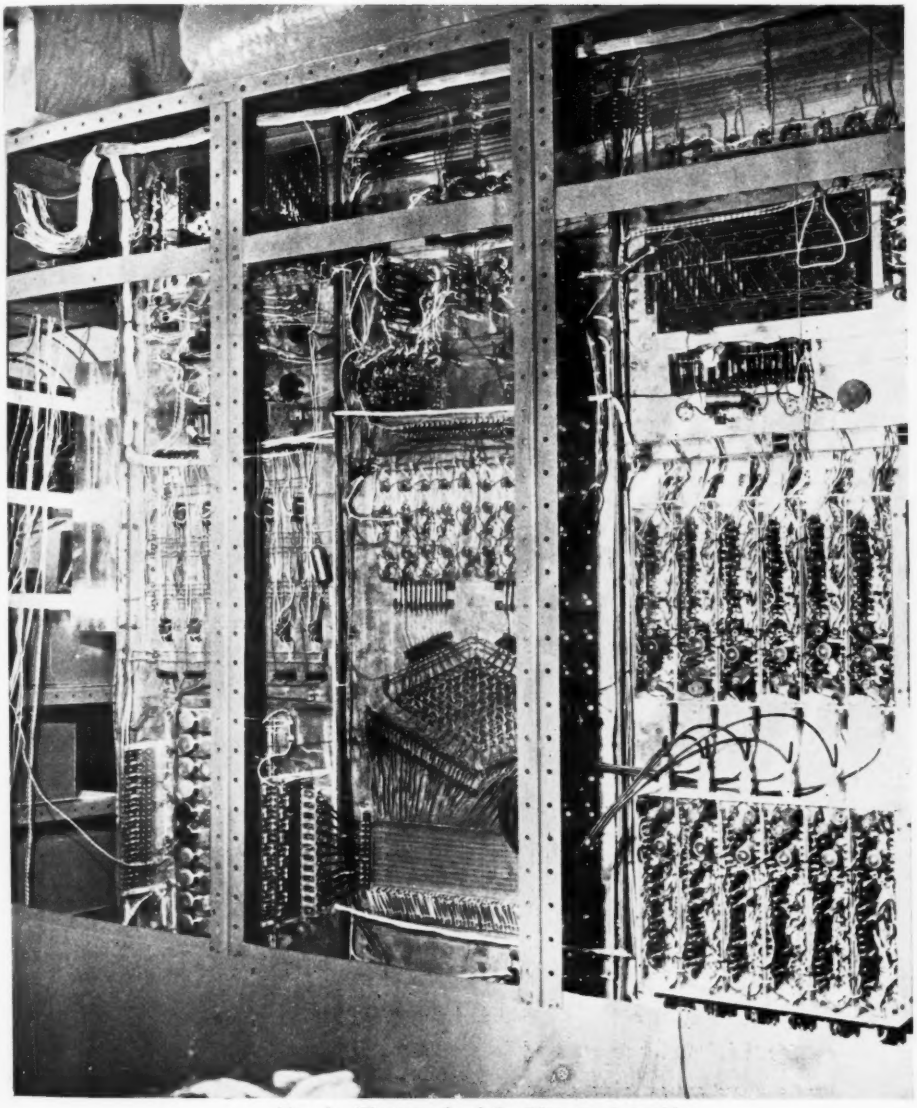

FIG. 1. Photograph of the Memory Assembly

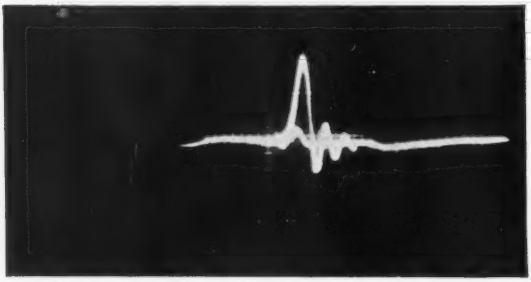

FIG. 7. Memory read out signals. Superimposed traces show 1 read out and 0 read out signals. The wanted (1 read out) signal amplitude is 100 mv.

STUDIES IN THE FORMATION OF HETEROCYCLIC RINGS CONTAINING NITROGEN

Part III. Condensation of 4-Methyl-*o*-Phenylenediamine with Aromatic Aldehydes

By N. V. Subba Rao and C. V. Ratnam

(*Department of Chemistry, Osmania University, Hyderabad-Dn.*)

Received January 28, 1957

(Communicated by Prof. T. R. Seshadri, F.A.SC.)

The reaction between 4-methyl-*o*-phenylenediamine and aromatic aldehydes was studied for the first time by Ladenburg[1] making use of benzaldehyde, anisaldehyde, and salicylaldehyde under different sets of conditions. The compound obtained from benzaldehyde was proved by Hinsberg[2] to be 1:2-disubstituted benziminazole, and that from anisaldehyde to possess analogous structure. However, Ladenburg (*loc. cit.*) could not prepare a similar compound when salicylaldehyde was used. He described in this case, the formation of two different compounds, one from one mole of the amine and three moles of aldehyde, and the other from two moles of amine and three moles of aldehyde, but could not assign definite structures to them. Hinsberg[3] through an extensive study of the reaction making use of aliphatic aldehydes reported the formation of 1:2-disubstituted benziminazoles from one mole of the amine and two moles of aldehyde occasionally accompanied by 2-mono-substituted benziminazoles. However, these workers left the position of the methyl group in the 1:2-disubstituted benziminazoles (5- or 6- position) uncertain. In a recent communication,[4] the present authors provided evidence to show that in these benziminazoles the methyl group occupied position 6 and not 5.

The condensation between 4-methyl-*o*-phenylenediamine and seventeen aromatic aldehydes has been studied making use of the modified Hinsberg's procedure,[5] and the results obtained are summarised in Table I. In a large measure, these results are in close agreement with those from simple *o*-phenylenediamine[5] and support the step-wise mechanism proposed earlier. In that communication it was shown that nucleophilic substituents in the aldehydes facilitate the exclusive formation of 1:2-disubstituted benziminazoles, while electrophilic groups favour the formation of monosubstituted compounds. The results presented in this paper further corroborate this view. Benzodiazepine derivatives could be isolated in condensations with benzaldehyde and *m*-nitrobenzaldehyde, and also with anisaldehyde. Monosub-

stituted benziminazoles could not, however, be obtained in the condensations with anisaldehyde, piperonal, and *p*-nitrobenzaldehyde. 5-Nitrosalicylaldehyde afforded a stable dianil under normal experimental conditions, and the corresponding benziminazole could be obtained only after refluxing it for twelve hours in acetic acid.

TABLE I

No.	Aldehyde condensed	Percentage yield of		
		1 : 2-Disubstituted benziminazole	2-Substituted benziminazole	Benzodiazepine derivative
1.	benzaldehyde	75*	18*	4*
2.	salicylaldehyde	95	..	..
3.	*m*-hydroxybenzaldehyde	95	..	..
4.	*p*-hydroxybenzaldehyde	82	..	..
5.	vanillin	70	..	..
6.	anisaldehyde	70*	..	4
7.	piperonal	95	..	..
8.	*o*-chlorobenzaldehyde	70	25*	..
9.	*p*-chlorobenzaldehyde	70	20	..
10.	2 : 4-dichlorobenzaldehyde	..	40	..
11.	3 : 4-dichlorobenzaldehyde	55	20	..
12.	*o*-nitrobenzaldehyde	50	38	..
13.	*m*-nitrobenzaldehyde	65	19	10
14.	*p*-nitrobenzaldehyde	82	..	..
15.	5-nitrosalicylaldehyde†	..	..	..
16.	*p*-dimethylaminobenzaldehyde ..	83	..	..
17.	1-naphthaldehyde	80	8	..

* Compounds already known in literature; † dianil was isolated in 95% yield.

EXPERIMENTAL

All m.p.'s are uncorrected. The microanalyses were carried out by one of the authors (C. V. R.). The percentage of nitrogen alone is recorded here since it is significant for deciding between the possible structures and not those of carbon and hydrogen.

General procedure for the condensation of 4-*methyl*-o-*phenylenediamine with aromatic aldehydes*

4-Methyl-*o*-phenylenediamine (one mole) and aromatic adlehyde (two moles) were dissolved separately in slight excess of glacial acetic acid, and mixed together in a conical flask, when evolution of heat was noticed. The

reaction was allowed to proceed at room temperature for one hour with occasional stirring. If any crystalline solid separated by this time, it was found to be generally a benzodiazepine derivative. This was separated by filtration, and the filtrate added to excess of crushed ice with vigorous stirring. The product obtained, if any, at this stage was found to be the 1 : 2-disubstituted benziminazole. The filtrate from this compound gave another substance on making it ammoniacal, which was either di- or mono-substituted benziminazole.

The condensation of 4-methyl-*o*-phenylenediamine with benzaldehyde has already been reported in our previous communication.[4]

1. 1-(o-*Hydroxybenzyl*)-2-(o-*hydroxyphenyl*)-6-*methyl benziminazole*.—4-Methyl-*o*-phenylenediamine was condensed with salicylaldehyde, and the acid solution was added to excess of crushed ice. The compound that separated was crystallised from alcohol, rectangular rods, m.p. 187° (Found: N, 8·2; $C_{21}H_{18}N_2O_2$ requires N, 8·5%). The acid filtrate, on making ammoniacal, yielded a small amount of the same substance.

2. 1-(m-*Hydroxybenzyl*)-2-(m-*hydroxyphenyl*)-6-*methyl benziminazole*.—The diamine was condensed with *m*-hydroxybenzaldehyde, and as no substance separated by the addition of the acid solution to crushed ice, the solution was made ammoniacal. The product obtained was the disubstituted benziminazole, which came out from alcohol in cubes, m.p. 245° (Found: N, 8·9; $C_{21}H_{18}N_2O_2$ requires N, 8·5%).

3. 1-(p-*Hydroxybenzyl*)-2-(p-*hydroxyphenyl*)-6-*methyl benziminazole*.—The diamine was condensed with *p*-hydroxybenzaldehyde, and the disubstituted benziminazole could be isolated from the ammoniacal solution as in 2 above. The product crystallised in needles from benzene, m.p. 185° (Found: N, 8·2; $C_{21}H_{18}N_2O_2$ requires N, 8·5%).

4. 1-(m-*Methoxy*-p-*hydroxybenzyl*)-2-(m-*methoxy*-p-*hydroxyphenyl*)-6-*methylbenziminazole*.—The diamine was condened with vanillin, and the disubstituted benziminazole could be isolated by making the dilute acid solution ammoniacal, just as in 2 and 3. It was purified by crystallisation from ethyl acetate, thin rectangular plates, m.p. 217° (Found: N, 7·6; $C_{23}H_{22}N_2O_4$ requires N, 7·2%).

5. 2 : 3 : 4-*Tri*-(p-*methoxyphenyl*)-7-(*or* 8)-*methyl benzodiazepine*.—The diamine was condensed with anisaldehyde, and the solid that separated from glacial acetic acid solution was filtered. It crystallised from alcohol in prismatic rods, m.p. 136° (Found: N, 5·9; $C_{31}H_{28}N_2O_3$ requires N, 5·9%).

6. 1-(p-*Methoxybenzyl*)-2-(p-*methoxyphenyl*)-6-*methyl benziminazole.*—The filtrate obtained after the separation of the diazepine derivative in the above condensation, was added to excess of crushed ice. The compound that separated was crystallised from alcohol, rectangular rods, m.p. 152°, and was found to be identical with that reported by Ladenburg.[1]

7. 1-(3:4-*Methylenedioxybenzyl*)-2-(3:4-*methylenedioxyphenyl*)-6-*methyl-benziminazole.*—The diamine was condensed with piperonal, and the acid solution was added to excess of crushed ice. The compound that separated was crystallised from petroleum ether (b.p. 60–80°), prismatic rods, m.p. 155° (Found: N, 7·4; $C_{23}H_{18}N_2O_4$ requires N, 7·3%). The filtrate, on making ammoniacal, gave a small amount of the same compound.

8. 1-(o-*Chlorobenzyl*-)-2-(o-*chlorophenyl*)-6-*methyl benziminazole.*—The diamine was condensed with *o*-chlorobenzaldehyde, and the acid solution was added to excess of crushed ice. The compound that separated was crystallised from petroleum ether, bundles of prismatic rods, m.p. 144°, (Found: N, 7·9; $C_{21}H_{16}N_2Cl_2$ requires N, 7·6%).

9. 2-(o-*Chlorophenyl*)-5-(*or* 6)-*methyl benziminazole.*—The filtrate obtained after the separation of the disubstituted benziminazole from the above condensation was made ammoniacal when the monosubstituted benziminazole separated. It crystallised from ethyl acetate in plates, m.p. 160°, and was identical with the one reported by Fischer.[6]

10. 1-(p-*Chlorobenzyl*)-2-(p-*chlorophenyl*)-6-*methyl benziminazole.*—4-Methyl-*o*-phenylenediamine was condensed with *p*-chlorobenzladehyde, and the acid solution was added to crushed ice. The compound that separated was crystallised from alcohol, rectangular rods, m.p. 160° (Found; N, 7·6; $C_{21}H_{16}N_2Cl_2$ requires N, 7·6%).

11. 2-(p-*Chlorophenyl*)-5-(*or* 6)-*methyl benziminazole.*—The filtrate obtained after the separation of the disubstituted benziminazole from the above condensation, was made ammoniacal, when the monosubstituted compound was obtained. It could be purified by recrystallisation from alcohol, rectangular plates, m.p. 221° (Found: N, 11·9; $C_{14}H_{11}N_2Cl$ requires N, 11·5%).

12. 2-(2:4-*Dichlorophenyl*)-5-(*or* 6)-*methyl benziminazole.*—The diamine was condensed with 2:4-dichlorobenzaldehyde, and the acid solution was added to excess of crushed ice. A low-melting solid was found to separate out, which on treatment with a small quantity of benzene or ethyl acetate, yielded a granular substance. The granular solid, on purification, gave the pure benziminazole needles from alcohol, m.p. 165° (Found: N, 10·5%;

$C_{14}H_{10}N_2Cl_2$ requires N, 10·1%). A small amount of the same compound was isolated by making the acid filtrate ammoniacal.

13. 1-(3 : 4-*Dichlorobenzyl*)-2-(3 : 4-*dichlorophenyl*)-6-*methyl benziminazole*.—The diamine was condensed with 3 : 4-dichlorobenzaldehyde and the acetic acid solution was added to crushed ice, when a sticky mass, which appeared to be a mixture, separated. The mass was treated with a little methanol, when a granular solid separated out. The granular solid, on recrystzllisation from alcohol, yielded the pure disubstituted benziminazole, bushy needles, m.p. 144° (Found: N, 6·3; $C_{21}H_{14}N_2Cl_4$ requires N, 6·4%).

14. 2-(3 : 4-*Dichlorophenyl*)-5-(*or* 6)-*methyl benziminzaole*.—The methanolic filtrate obtained after the separation of the disubstituted benziminazole given above, on concentration, gave a resinous mass. It was repeatedly crystallised from alcohol and finally from ethyl acetate to yield the pure monosubstituted compound, rectangular rods, m.p. > 300° (Found: N, 10·2; $C_{14}H_{10}N_2Cl_2$ requires N, 10·1%).

15. 1-(o-*Nitrobenzyl*)-2-(o-*nitrophenyl*)-6-*methyl benziminazole*.—4-Methyl-*o*-phenylenediamine was condensed with *o*-nitrobenzaldehyde, and the acid solution was added to excess of crushed ice. A resinous mass separated out, which on repeated crystallisation from alcohol, gave the pure benziminazole, yellow microcrystalline solid, m.p. 135° (Found: N, 14·5; $C_{21}H_{16}N_4O_4$ requires N, 14·4%).

16. 2-(o-*Nitrophenyl*)-5-(*or* 6)-*methyl benziminazole*.—The acid filtrate from above was made ammoniacal when the monosubstituted benziminazole separated out. It was crystallised from alcohol, yellow rectangular plates, m.p. 214° (Found: N, 16·6; $C_{14}H_{11}N_3O_2$ requires N, 16·6%).

17. 2 : 3 : 4-*Tri*-(m-*nitrophenyl*)-7-(*or* 8)-*methyl benzodiazepine*.—The diamine was condensed with *m*-nitrobenzaldehyde, and the compound that separated from glacial acetic acid solution was filtered. It was crystallised from benzene, orange-red plates, m.p. 170° (Found: N, 13·5; $C_{28}H_{19}N_5O_6$ requires N, 13·4%).

18. 1-(m-*Nitrobenzyl*)-2-(m-*nitrophenyl*)-6-*methyl benziminazole*.—The acid filtrate obtained after the separation of the diazepine derivative from the above condensation, was added to excess of crushed ice. The compound that separated was crystallised from alcohol, tiny yellow rods, m.p. 157° (Found: N, 14·5; $C_{21}H_{16}N_4O_4$ requires N, 14·4%).

19. 2-(m-*Nitrophenyl*)-5-(*or* 6)-*methyl benziminazole*.—The dilute acid filtrate obtained after the separation of the disubstituted benziminazole in *m*-nitrobenzaldehyde condensation, was made ammoniacal, when an yellow

solid was obtained. It crystallised from alcohol in yellow clusters of needles m.p. 195° (Found: N, 16·3; $C_{14}H_{11}N_3O_2$ requires N, 16·6%).

20. 1-(p-*Nitrobenzyl*)-2-(p-*nitrophenyl*)-6-*methyl benziminazole*.—The diamine was condensed with *p*-nitrobenzaldehyde, and the acid solution was added to crushed ice, when an yellow substance separated. It was crystallised from alcohol, yellow needles, m.p. 193° (Found: N, 14·7; $C_{21}H_{16}N_4O_4$ requires N, 14·4%).

21. *Bis*-(5-*nitrosalicylidene*)-*tolylene*-3: 4-*diamine*.—A solution of 5-nitrosalicylaldehyde in glacial acetic acid was added to a similar solution of 4-methyl-*o*-phenylenediamine, when an orange-yellow solid immediately separated. It was sparingly soluble in the common organic solvents, and could be crystallised from hot nitrobenzene in orange needles, m.p. 215° (Found: N, 13·4; $C_{21}H_{16}N_4O_6$ requires N, 13·3%).

22. 1-(2-*Hydroxy*-5-*nitrobenzyl*)-2-(2-*hydroxy*-5-*nitrophenyl*)-6-*methyl benziminazole*.—The above dianil was refluxed in glacial acetic acid for a period of twelve hours. The solution was diluted, filtered, and the filtrate was made ammoniacal. An yellow compound that separated, on crystallisation from benzene, yielded the pure benziminazole, yellow microcrystalline solid, m.p. 286° (decomp.) (Found: N, 13·3; $C_{21}H_{16}N_4O_6$ requires N, 13·3%).

23. 1-(p-*Dimethylaminobenzyl*)-2-(p-*dimethylaminophenyl*)-6-*methyl benziminazole*.—The diamine was condensed with *p*-dimethylaminobenzaldehyde at 100° for one hour, since the reaction did not proceed at room temperature. The acid solution, on addition to crushed ice, did not give any precipitate, and therefore it was made ammoniacal. The compound that separated was crystallised from benzene, prismatic rods, m.p. 248° (Found: N, 15·1; $C_{25}H_{28}N_4$ requires N, 14·6%).

24. 1-(1-*Naphthyl methyl*)-2-(1-naphthyl)-6-*methyl benziminazole*.—4-Methyl-*o*-phenylenediamine was condensed with 1-naphthaldehyde by the general method, and the acetic acid solution was added to excess of crushed ice. The compound that separated was crystallised from benzene-petroleum ether, prismatic rods, m.p. 172°, (Found: N, 6·7; $C_{29}H_{22}N_2$ requires N, 7·0%).

25. 2-(1-*Naphthyl*)-5-(*or* 6)-*methyl benziminazole*.—The filtrate obtained after the separation of the disubstituted benziminazole from the above condensation was made ammoniacal, and the compound that separated was recrystallised from alcohol, prismatic rods, m.p. 233° (Found: N, 10·6; $C_{18}H_{14}N_2$ requires N, 10·9%).

Summary

The reaction between 4-methyl-*o*-phenylene diamine and seventeen aromatic aldehydes has been investigated, and twenty-three new compounds obtained have been characterised. The results are in close agreement with those from *o*-phenylenediamine and aromatic aldehydes, and corroborate the inferences drawn regarding the influence of substituents in the aldehydes on the mode of the reaction and cyclisation.

References

1. Ladenburg .. *Ber.*, 1877, **10**, 1123; 1878, **11**, 590, 1656.
2. Hinsberg .. *Ibid.*, 1886, **19**, 2025.
3. ———— .. *Ibid.*, 1887, **20**, 1585.
4. Rao and Ratnam .. *Proc. Ind. Acad. Sci.*, 1956, **64**, 331.
5. ———— .. *Ibid.*, 1956, **63**, 173.
6. Fischer .. *J. Prakt. Chem.*, 1924, **107**, 16; *C.A.*, 1924, **18**, 1652.

HETEROCYCLIC COMPOUNDS

Part IX.* Synthesis of a Quinoline Lactone

By P. S. Raman

(*Department of Organic Chemistry, University of Madras, Madras-25*)

Received March 4, 1957

(Communicated by Dr. K. N. Menon, F.A.SC.)

THE chemistry of furano-quinolines is of interest from the point of view of alkaloid chemistry. This laboratory has been paying some attention to work out simple methods for synthesising members of this group and although the scheme is not complete, the synthesis of some of the compounds obtained are placed on record. Acetoacetanilide (I) forms a sodio-derivative very readily when heated with molecular sodium, which undergoes condensation with alkyl halides and halogenated aliphatic esters. Reaction with bromo-acetic ester gave (II) which could be readily ring closed with concentrated sulphuric acid to give 2-hydroxy-4-methyl-quinoline-3-acetic acid (III). The lactam acid so formed is easily soluble in bicarbonate solution, but insoluble in dilute acids. On heating with acetic anhydride it readily afforded the lactone (IV). The lactonic nature of the product is proved by analysis and by its conversion into the methyl and ethyl esters of (III). Unlike in the benzene analogues, compound (IV) does not react normally with phosphorous halides, evidently due to the influence of the nitrogen in the ring system.

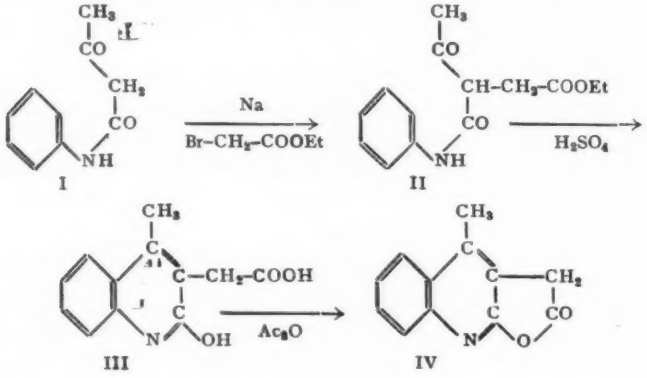

I II III IV

* Part VIII: *Proceedings*, Vol. XLIV, No. 3. Sec. A, 1956.

Experimental

Acetoacetanilide (I) was prepared according to the method of Hauser and Reynolds (*J. Amer. Chem. Soc.*, 1948, **70**, 2402). The anilide (4·5 gm.) was dissolved in hot, pure, dry benzene (50 ml.) and to it was added molecular sodium (0·6 gm.) suspended in benzene. A vigorous reaction ensued and after this had subsided, the mixture was refluxed under exclusion of moisture till effervescence ceased (5–6 hours). The mixture was cooled to room temperature and after addition of freshly distilled bromoacetic ester (3 c.c.) was refluxed for two hours. It was then cooled, treated with ice-water and the benzene layer separated. The aqueous layer was extracted with benzene once, the combined benzene solutions washed with water, dried over anhydrous sodium sulphate, and the benzene removed. The product (II), which was a thick brownish liquid, proved difficult to purify. It was treated with concentrated sulphuric acid (20 ml.) with cooling. The resulting solution was left to stand at the room temperature for 20 hours, then heated on the water-bath for 30–40 minutes, cooled and poured on to ice. The resulting fine precipitate was dissolved in bicarbonate and reprecipitated yielding 4 gm. of (III). The acid is insoluble in hot alcohol and very sparingly soluble in hot acetone. It crystallised from hot acetic acid in colourless, small, rectangular prisms of m.p. 285° (decomp.). Found: C, 65·73, H, 5·08; $C_{12}H_{11}O_3N$ requires 66·36 and 5·07 respectively.

The Lactone—IV

The acid (0·8 gm.) was heated with acetic anhydride (2 ml.) in an oil-bath at 100–05° for 4 hours, the cooled mixture diluted with ice-water, stirred well and the solid collected. It was stirred with cold bicarbonate solution, the insoluble portion collected (0·7 gm.) and crystallised from acetone. It separated in the form of thick, stout, yellowish rods, m.p. 206–08° (decom.) when introduced into a pre-heated bath. Found: C, 72·69, H, 4·54, $C_{12}H_9O_2N$ requires 72·36 and 4·52. The lactone is insoluble in cold bicarbonate, but dissolves slowly on shaking with cold, dilute caustic alkali. It is readily converted into the acid even on boiling with aqueous acetic acid. On boiling with absolute methyl alcohol it is converted into the methyl ester of the acid. The ester was prepared by refluxing the lactone with methyl alcohol for an hour. On cooling the ester crystallised out. The ethyl ester was similarly prepared. Recrystallised from ethanol, it separated in the form of needles, m.p. 223–25°. Found: C, 68·87, H, 6·41; $C_{14}H_{15}O_3N$ requires 68·57 and 6·12.

ACKNOWLEDGEMENT

This work arose from some schemes drawn up by Dr. K. N. Menon to synthesise members of the Dictamnine group. The author is very grateful to Dr. Menon for guidance and help.

OPTICAL PROPERTIES AND UNIT CELL PARAMETERS OF NICKEL NITRATE HEXAHYDRATE

By A. Jayaraman, F.A.Sc.

(*Memoir No. 95 of the Raman Research Institute, Bangalore-6*)

Received March 30, 1957

1. Introduction

Nickel nitrate is known to form three hydrates with three, six and nine molecules of water at 55° C., — 16° C. and — 27° C. respectively. Very little is known regarding the structure and physical properties of these hydrates. Groth in his *Chemische Crystallographie* reports some measurements of interfacial angles, axial ratios, density and melting point of nickel nitrate hexahydrate. The hexahydrate is reported to occur as green deliquescent crystals having a density of 2·05 gm./c.c. in the monoclinic prismatic class with axial ratios $a:b:c = 1{\cdot}164:1:1{\cdot}905$ and $\beta = 101° 26'$. In the literature as far as the author could find, the structure and optical properties of this substance has not been reported. Further it would be of particular interest to study the magnetic properties of single crystals of this substance. It should however be borne in mind that the material is of a highly hygroscopic nature and hence needs special technique of study. It was with a view to understand the structure and optical properties of this substance, that the present investigation was undertaken and the results of study are reported in the present communication. It would be in place to mention here that the crystals of hexahydrate obtained by the author could only be placed in the triclinic system as the optical and X-ray investigations unequivocally show this to be the case. This is in contrast to the previous report quoted earlier.

2. Experimental Study

Crystals of nickel nitrate hexahydrate for both optical and X-ray work were grown from a purified commercially available sample. The solubility of this substance is very high in water and is considerable in many organic compounds, particularly alcohol and acetone. A saturated solution in water of the substance was kept inside an airtight bell jar in a crystallising dish along with a small quantity of P_2O_5 or anhydrous calcium chloride in a separate container which served to absorb water. It was observed that crystals of

large size could be grown by this method. Since the crystals are extremely deliquescent, they were taken out of the mother liquor and transferred promptly to a bottle containing kerosene after the adhering solution was removed between blotting papers.

Needle-shaped crystals were obtained by rapid crystallisation while large elongated plates were obtained by slower crystallisation. The crystals were of a beautiful emerald green in colour and well developed crystallographic faces could be observed in it. Visual examination of the morphological characters revealed that the crystals did not possess any element of symmetry and the form was suggestive of a triclinic pinacoidal type. In very well developed crystals, many other faces could be discerned. However an optical goniometric study was not attempted as this would necessitate special immersion methods.

3. CELL PARAMETERS

Rotation and zero-layer Weissenberg X-ray photographs were taken with thin rods cut parallel to the three observed edges of the crystal form. Considerable difficulty was experienced in handling the specimens, cutting them parallel to the chosen edges, and shaping them to correct thickness owing to the extreme hygroscopic nature of the material. The rod-shaped specimen was placed in a thin-walled pyrex capillary tube, sealed at one end while the other open end was closed with wax and mounted on the goniometer head. Cu Kα radiation was employed to record the X-ray patterns. The following linear dimensions of the unit cell and its angular constants were obtained from the three single crystal and the three zero-layer Weissenberg photographs. With these six photographs cross checks of the data were possible.

$$a = 5{\cdot}79 \text{ Å.U.} \qquad \alpha = 106°{\cdot}38'$$
$$b = 7{\cdot}69 \text{ Å.U.} \qquad \beta = 80°{\cdot}32'$$
$$c = 11{\cdot}89 \text{ Å.U.} \qquad \gamma = 101°{\cdot}27'$$
$$a : b : c = 0{\cdot}753 : 1 : 1{\cdot}546$$

The density of the material was found to be about 2 gm./c.c. and the number of molecules per unit cell when calculated came out very close to 2, revealing thereby that there are two molecules per unit cell.

In the convergent light figure observed with the cleavage plate of the crystal the brush is quite dark and very distinct while crossing the eyes, thereby indicating that the crystal is not optically active. Further, when copper radiation is used for recording the X-ray patterns, one is working very close

to the absorption edge of nickel, a favourable circumstance for the breakdown of Friedel's law if there were no centre of symmetry. No such breakdown was noticeable in the X-ray photographs and therefore it is highly probable that the crystal belongs to the centro-symmetric class of the triclinic system, the corresponding space group symobl being C_i^1 or $P\bar{1}$.

It should be remarked here that the crystal exhibits a very perfect (001) cleavage. The needle axis is found to be 5·79 A.U. while the *c*-axis is 11·89 A.U.

4. Optical Properties

The optical properties of the crystal were determined with the help of a polarising microscope. The habit plane of the crystal which is found to be the (010) face by X-ray methods exhibits straight extinction. The cleavage plate which is found to be parallel to the (001) face gives an inclined extinction, the vibration direction making an angle of 11° with the straight edge of the crystal which is parallel to the *a*-axis (100).

The convergent light figure is observed on the (001) face that is the cleavage plate and the β vibration direction lies on this. The optic axial angle was determined by adopting the undermentioned procedure which was found to be very convenient. The cleavage plate was mounted between a glass plate and a cover slip with a suitable immersion liquid and this was placed on a Federov stage. The stage was fixed on to a polarising microscope and a glass hemisphere belonging to the Federov stage was attached to the stage of the microscope in the aperture admitting light. This acted as a converging lens and with a low power objective and the Betrand lens one could easily observe the interference figure. The crystal could easily be set by proper adjustment of the stage such that the axial plane is brought parallel to one of the cross wires. Having obtained this setting, the axial angle is easily determinable and two principal refractive indices could also be obtained. For obtaining the latter, parallel light is needed which can be got by removing the hemispherical glass condenser and lowering the substage, while leaving the desired setting of the crystal undisturbed.

The axial angle and the two refractive indices β and γ were obtained by following the above procedure and using immersion methods to measure the refractive index. The third principal refractive index (α) was measured on the (010) face by suitably tilting the stage to get the vibration direction parallel to the cross wire. The following are the values obtained for sodium light.

$\alpha = 1{\cdot}422$

$\beta = 1{\cdot}555$ $\qquad 2\,V = 41°{\cdot}12'$

$\gamma = 1{\cdot}577$

A diagram is reproduced below to show the orientation of the optic elements with respect to the crystallographic elements observed in the crystal. The acute bisectrix is the (α) vibration direction and the crystal is therefore biaxial negative.

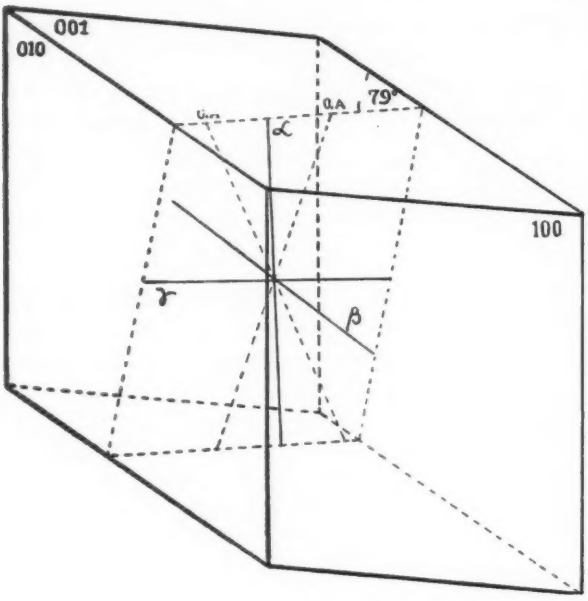

FIG. 1

As already remarked, crystals of $Ni(NO_3)_2\,6H_2O$ are emerald green in colour and exhibit pleochroism in polarised light. Pleochroism is very striking on the (010) face. For a vibration parallel to (α) the colour is bluish green while it is yellowish green for a vibration parallel to the (β) vibration direction. Pleochroism is not marked on the cleavage face and the difference in absorption is not observable for a vibration parallel to β and γ vibration directions.

5. SOME REMARKS

A study of the optical properties in relation to the observed morphological characters of the crystal by itself revealed that the crystal can only

be placed in the triclinic system. The straight extinction observed can only be an accident the possibility of which is not totally excluded for a cyrstal belonging to the triclinic system. Otherwise, the optical properties bear no symmetric relationship to the crystal edges and faces.

It would be seen from an examination of refractive index data that the maximum refractive index lies very close to the cleavage plane and the minimum index is nearly normal to it. The difference between the two indices, *i.e.*, the birefringence, is fairly high. The perfect cleavage of the (001) plane and the refractive properties indicate that the planar nitrate ions lie very close to the cleavage plane.

A complete determination of the structure and other physical properties is under progress and the results will be reported in due course.

In conclusion the author wishes to express his thanks to Sir C. V. Raman, F.R.S., N.L., for his kind interest in the work and to Dr. S. Ramaseshan for helpful criticisms.

Summary

The unit cell parameters and optical properties of nickel nitrate hexahydrate are reported. It is found that the crystal belongs to the centrosymmetric class in the triclinic system. The refractive properties and the very perfect cleavage of the (001) indicate that the planar nitrate ions lie very close to the (001) face.

NUMERICAL CALCULATIONS ON THE NEW APPROACH TO THE CASCADE THEORY—II

By S. K. Srinivasan and N. R. Ranganathan

(*Department of Physics, University of Madras, Madras, India*)

Received January 28, 1957

(Communicated by Dr. Alladi Ramakrishnan, F.A.SC.)

Abstract

Numerical results on the mean numbers of electrons produced in small thicknesses in a shower initiated by a single electron are presented on the basis of the new approach to the cascade theory.

In a recent contribution to these *Proceedings*, Ramakrishnan and one of us (S. K. S.) (1956) have suggested a new approach to the cascade theory. In a subsequent contribution (1957, hereinafter referred to as Paper I), we have presented numerical results on the mean numbers of electrons produced for large thicknesses. We here deal with the mean numbers for small thicknesses.

The mean number of electrons produced between 0 and t with the energy of each electron being $> E_c$ at the point of its production can be written as

$$\epsilon\{N(y;t)\} = \frac{1}{2\pi i}\int_{\sigma-i\infty}^{\sigma+i\infty}\frac{B_s C_s}{\mu_s-\lambda_s}\cdot\frac{e^{y(s-1)}}{s-1}\left[\left(\frac{1}{\lambda_s}-\frac{1}{\mu_s}\right)-\left(\frac{e^{-\lambda_s t}}{\lambda_s}-\frac{e^{-\mu_s t}}{\mu_s}\right)\right]ds \quad (1)$$

where $y = \log E_0/E_c$ and A_s, B_s, C_s, λ_s and μ_s are defined in Paper I. For small thicknesses, we cannot neglect the term containing $e^{-\mu_s t}/\mu_s$ as has been done in Paper I. But the term

$$\frac{1}{2\pi i}\int_{\sigma-i\infty}^{\sigma+i\infty}e^{y(s-1)}\frac{B_s C_s}{\mu_s-\lambda_s}\frac{e^{-\mu_s t}}{\mu_s}\frac{}{(s-1)}ds$$

does not have any saddle point and hence cannot be evaluated in the same manner as in Paper I. This can be done if we adopt the device of re-grouping the terms in (1) as

$$\epsilon\{N(y;t)\} = \epsilon\{N_\lambda(y;t)\} - \epsilon\{N_\mu(y;t)\} \quad (2)$$

where

$$\epsilon\{N_\lambda(y;t)\} = \frac{1}{2\pi i}\int_{\sigma-i\infty}^{\sigma+i\infty} \frac{B_s C_s}{\mu_s - \lambda_s} \cdot \frac{e^{y(s-1)}}{\lambda_s (s-1)}\, ds$$

$$- \frac{1}{2\pi i}\int_{\sigma-i\infty}^{\sigma+i\infty} \frac{B_s C_s}{\mu_s - \lambda_s} \cdot \frac{e^{-\lambda_s t + y(s-1)}}{\lambda_s (s-1)}\, ds \tag{3}$$

$$\epsilon\{N_\mu(y;t)\} = \frac{1}{2\pi i}\int_{\sigma-i\infty}^{\sigma+i\infty} \frac{B_s C_s}{\mu_s - \lambda_s} \frac{e^{y(s-1)}}{s-1}\left(\frac{1 - e^{-\mu_s t}}{\mu_s}\right) ds \tag{4}$$

$\epsilon\{N_\lambda(y;t)\}$ can be evaluated in the same manner as has been done in Paper I.

To evaluate $\epsilon\{N_\mu(y;t)\}$ we adopt the following procedure. Since we are interested only in small thicknesses, the term $(1 - e^{-\mu_s t})/\mu_s$ can be expanded and we need retain the first three or four terms of the expansion. Thus to a very good approximation we can write

$$\epsilon\{N_\mu(y;t)\} = \sum_{m=0}^{4} \frac{I_m\, t^{m+1}}{(m+1)!} \tag{5}$$

where

$$I_m = \frac{1}{2\pi i}\int_{\sigma-i\infty}^{\sigma+i\infty} e^{\chi_m(s)}\, ds \tag{6}$$

$$\chi_m(s) = \log \frac{B_s C_s}{\mu_s - \lambda_s} - \log(s-1) + m \log \mu_s + y(s-1) \tag{7}$$

As s tends to $+1$, it is easy to see that $\chi_m(s)$ tends to $+\infty$ since C_s tends to $+\infty$ as s tends to $+1$. As s tends to $+\infty$, through real values it can be proved, as has been done in Paper I that $\chi_m(s)$ tends to $+\infty$ and that I_m has a saddle point s_0. We obtain the formula

$$I_m = \frac{e^{\chi_m(s_0)}}{\sqrt{2\chi_m''(s_0)}} \tag{8}$$

where s_0 is the saddle point given by

$$\left(\frac{d\chi_m(s)}{ds}\right)_{s=s_0} = 0. \tag{9}$$

The mean numbers corresponding to $t = 0{\cdot}5$ and $t = 0{\cdot}8$ have been calculated for various values of y. In this case, the saddle points fall between $s = 1$ and $s = 2$. *In this interval the basic functions cannot be obtained by sub-tabulation from any of the standard cascade tables due to the fact that C_s, λ_s and μ_s become infinite at $s = 1$.* Hence it is considered worthwhile to tabulate these functions from their definitions and these are given in Table I. Table II gives the mean number of electrons produced

TABLE I

S	A_s	B_s	C_s	λ_s	μ_s
1·1	·152041	1·400998	12·821039	3·786712	4·712431
1·12	·180151	1·375115	10·575366	3·348058	4·301886
1·14	·207592	1·350215	8·975642	3·002095	3·983364
1·16	·234398	1·326244	7·779412	2·719330	3·727407
1·18	·260595	1·303151	6·851997	2·482030	3·516303
1·2	·286213	1·280890	6·112601	2·278786	3·338677
1·22	·311253	1·259418	5·509812	2·101890	3·186821
1·24	·335756	1·238694	5·009375	1·945888	3·055322
1·26	·359742	1·218679	4·587573	1·806813	2·940233
1·28	·383234	1·199349	4·227471	1·681704	2·838617
1·3	·406253	1·180640	3·916663	1·568256	2·748187
1·32	·428816	1·162552	3·645837	1·464717	2·667211
1·34	·450943	1·145050	3·407887	1·369668	2·594289
1·36	·472649	1·128091	3·197285	1·281956	2·528284
1·38	·493951	1·111666	3·009666	1·200662	2·468291
1·4	·514864	1·095745	2·841548	1·125010	2·413552
1·42	·535401	1·080305	2·690106	1·054357	2·363437
1·44	·555577	1·065325	2·553038	·988160	2·317415
1·46	·575404	1·050785	2·428441	·925958	2·275040
1·48	·594894	1·036665	2·314730	·867356	2·235928
1·5	·614060	1·022949	2·210578	·812012	2·199750
1·52	·632911	1·009618	2·114858	·759632	2·166221

TABLE I (*contd.*)

S	A_s	B_s	C_s	λ_s	μ_s
1·54	·651458	·996656	2·026617	·709956	2·135092
1·56	·669712	·984050	1·945035	·662759	2·106149
1·58	·687681	·971783	1·869409	·617841	2·079200
1·6	·705375	·9598433	1·799129	·575026	2·054079
1·62	·722802	·948217	1·733663	·534155	2·030635
1·64	·739970	·936892	1·672550	·495088	2·008736
1·66	·756888	·925857	1·615383	·457698	1·988264
1·68	·773562	·915101	1·561801	·421874	1·969113
1·7	·790001	·904612	1·511491	·387511	1·951189
1·72	·806210	·894383	1·464169	·354517	1·934405
1·74	·822196	·884401	1·419587	·322809	1·918683
1·76	·837966	·874659	1·377520	·292309	1·903953
1·78	·853526	·865148	1·337768	·262948	1·890152
1·8	·868881	·855860	1·300152	·234663	1·877222
1·82	·884037	·846788	1·264509	·207393	1·865108
1·84	·899000	·837922	1·230692	·181084	1·853762
1·86	·913773	·829258	1·198570	·155689	1·843140
1·88	·928364	·820786	1·168023	·131159	1·833201
1·9	·942775	·812502	1·138941	·107455	1·823907
1·92	·957012	·804399	1·111223	·084534	1·815224
1·94	·971079	·796470	1·084780	·062360	1·807117
1·96	·984979	·788711	1·059528	·040901	1·799558
1·98	·998719	·781115	1·035392	·020124	1·792521
2	1·012300	·773678	1·012300	0	1·785978

for $t = 0{\cdot}5$ and $t = 0{\cdot}8$. For comparison we have also tabulated the mean number of electrons that exist at t given by standard cascade theory.

TABLE II

Mean numbers for small thicknesses

	y	$\epsilon\{N_\lambda(y;t)\}$	$\epsilon\{N_\mu(y;t)\}$	$-\epsilon\{N(y;t)\}$ [$\epsilon\{n(y;t)\}$* is given in brackets]
$t = 0{\cdot}5$	8	20·6	·532	20·1† (2·62)
	7	10·2	·503	9·70†(2·33)
	6	5·1	·445	4·66 (2·08)
	5	2·73	·459	2·27 (1·78)
$t = 0{\cdot}8$	8	35·7	·670	35·0† (4·93)
	7	16·7	·617	16·1† (4·13)
	6	8·65	·430	8·22 (3·40)
	5	4·59	·556	4·03 (2·74)

We are deeply indebted to Dr. Ramakrishnan for suggesting this programme of work. We are grateful to the University of Madras for the grant of a Government of India Senior Scholarship to one of us (S. K. S.) and a studentship for the other (N. R. R.).

Note.—In a private communication, Dr. Fay at Gottingen has pointed out that our values for $\epsilon\{N(y;t)\}$ are too large in the case of $y = 7$ and 8 (indicated by † in Table II) as compared with his experimental data. We are inclined to agree with him and admit that the technique we have adopted of splitting the terms in equation (3) is not suitable for large values of y and small t. In (3), $\epsilon\{N_\lambda(y;t)\}$ is given by the difference of two terms and since each of these terms is large and their difference is small, we cannot assert that the computed differences are accurate. We admit that our method is unsuitable in such cases though it yields very good results for all other cases. The results for large y and small t are presented to invite an improvement to our technique.

REFERENCES

1. Ramakrishnan, Alladi and Srinivasan, S. K. — *Proc. Ind. Acad. Sci.*, 1956, **44 A**, 263.
2. Srinivasan, S. K. and Ranganathan, N. R. — *Ibid.*, 1957, **45 A**, 69.

* $\epsilon\{n(y;t)\}$ denotes the mean number of electrons that exist at t.

422–57. Printed at The Bangalore Press, Bangalore City, by C. Vasudeva Rao, Superintendent, and Published by The Indian Academy of Sciences, Bangalore.

NOTICE TO AUTHORS

Scientific papers intended for publication in the *Proceedings of the Indian Academy of Sciences* can be accepted only when they are communicated by a Fellow of the Academy whose duty shall be to satisfy himself that such communications are fit to be read at the Meeting of the Academy and published in its *Proceedings*.

Papers should not ordinarily exceed fifty pages of foolscap. MSS. should be either typewritten or written in legible hand on one side of the paper. All papers should be carefully revised by the authors and should be absolutely in final form for printing. Position for text-figures should be indicated. Each paper shall conclude with a critical summary not exceeding 350 words.

Drawings, diagrams or other illustrations should be made on larger scale (preferably) twice the size than the ones in which they are intended to appear. They should be done in Indian ink on bristol board with lettering in pencil. Scale of magnification of camera lucida tracings should be indicated by the side of drawings. In certain special cases arrangements will also be made for monochrome lithographic and other colour plates. Reduction of illustrations desired should be indicated in pencil. Appropriate legends should accompany all drawings. Names of authors are to be marked in pencil on the left-hand corner of drawing sheets. Photomicrographs should be securely mounted with colourless paste.

All tables, quotations and footnotes which will be set hereafter (beginning from Vol. I, No. 2) in types smaller than the text, should be typewritten on separate sheets and placed with the text in proper sequence. Footnotes should be numbered in Arabic numerals.

References to literature in the text should be given, whenever possible, in chronological order, only the names of authors and years of publication, in brackets, being given. They should be cited in full after the summary, the authors' names following in alphabetical order. Thus,

Name or Names of author; Name of Journal (abbreviation) with a single underline; Year of publication; Number of Volume with a double underline, and lastly page. The following would be a useful illustration:—

Bergmann and Stather . . . . . Z. Physiol. Chem., 1926, 152, 189.

Two copies of slip-proof and wherever possible, a page proof for final revision will be sent to authors. All corrections are best made on the slip-proof which should be transmitted to the Office of the Academy. All proof corrections involve heavy expenses which would be negligible if the papers are carefully revised by the authors before submission.

Fifty free reprints including plates and with cover will be supplied for each paper. Additional copies can be supplied at cost on previous intimation.

Blocks appearing in the *Proceedings* will be available for purchase by their respective authors. Orders for the same should be sent along with the corrected proofs and in any case not later than one month after the date of publication of the paper. The price charged would be 25% of the actual cost of the blocks *plus* freight and despatching charges. If the blocks are reproduced in other journals or publications, due acknowledgment should be made in them to the *Proceedings*.

The original drawings and plates of blocks appearing in the *Proceedings* will be returned to such of the authors as may require them provided the cost of despatching such originals is borne by them.

CONTENTS

PAGE

On a Time of Flight Method of Studying the Velocity Distribution of Neutrons from Diffusing Media . V. C. Deniz, S. B. D. Iyengar and R. Ramanna 205

Slowing Down and Diffusion of Neutrons in Beryllium Oxide . . . . . S. B. D. Iyengar, G. S. Mani, R. Ramanna and N. Umakanth 215

Temperature Dependence of the Slowing Down and Diffusion Constants of Neutrons in Beryllium Oxide . . . . . S. B. D. Iyengar, G. S. Mani, R. Ramanna and N. Umakanth 224

The Input and Output System of the T.I.F.R. Computer . . . . . B. K. Basu and K. Bakhru 231

A Two Dimensional Ferrite-Core Memory . . . . . M. M. Farooqui, S. P. Srivastava and R. N. Neogi 240

Studies in the Formation of Heterocyclic Rings Containing Nitrogen. Part III. Condensation of 4-Methyl-*o*-Phenylenediamine with Aromatic Aldehydes . . . . . N. V. Subba Rao and C. V. Ratnam 253

Heterocyclic Compounds. Part IX. Synthesis of a Quinoline Lactone . . . . . P. S. Raman 260

Optical Properties and Unit Cell Parameters of Nickel Nitrate Hexahydrate . . . . . A. Jayaraman 263

Numerical Calculations on the New Approach to the Cascade Theory—II . . . . . S. K. Srinivasan and N. R. Ranganathan 268

PAGE
205
215
224
231
240
253
260
263
268